Enhancing the Stability of Albumin Foam-based Support Baths using Pectin for Embedded Bioprinting

by

Melanie RODGER

MANUSCRIPT-BASED THESIS PRESENTED TO ÉCOLE DE TECHNOLOGIE SUPÉRIEURE IN PARTIAL FULFILLMENT OF A MASTER'S DEGREE WITH THESIS IN MECHANICAL ENGINEERING
M.A.Sc.

MONTREAL, DECEMBER 2, 2025

ÉCOLE DE TECHNOLOGIE SUPÉRIEURE
UNIVERSITÉ DU QUÉBEC

BOARD OF EXAMINERS

THIS THESIS HAS BEEN EVALUATED

BY THE FOLLOWING BOARD OF EXAMINERS

Mr. Ali Ahmadi, Thesis supervisor
Department of Mechanical Engineering, École de technologie supérieure

Mr. Giuseppe Di Labbio, Chair, Board of Examiners
Department of Mechanical Engineering, École de technologie supérieure

Ms. Nicole Demarquette, Member of the Jury
Department of Mechanical Engineering, École de technologie supérieure

Mr. Joseph Matt Kinsella, External Examiner
Department of Bioengineering, McGill University

THIS THESIS WAS PRESENTED AND DEFENDED

IN THE PRESENCE OF A BOARD OF EXAMINERS AND THE PUBLIC

ON NOVEMBER 4, 2025

AT ÉCOLE DE TECHNOLOGIE SUPÉRIEURE

DEDICATION

To my parents,

for always believing in me.

ACKNOWLEDGEMENTS

First and foremost, I would like to express my deepest gratitude to my supervisor, Dr. Ali Ahmadi. From first welcoming me into his lab in 2017, when I was still in high school, to guiding me throughout the course of this master's thesis, he has been a constant source of encouragement, mentorship, and support. His patience and insight have not only helped me grow as a researcher but also enabled me to overcome challenges along the way, for which I am truly grateful.

Further, I would like to thank all of my lab mates that I have had the pleasure of working with over the past couple years. Being a member of the BBF Lab has been an honour and I am very thankful to have been surrounded by such a friendly and supportive group of people.

To my family, thank you for your unconditional love, support, and encouragement throughout my academic journey. Your belief in me has been a constant source of strength, and your patience and understanding during the most demanding times made all the difference.

Lastly, I would like to acknowledge the funding that has supported my research throughout my master's program including Natural Sciences and Engineering Research Council of Canada (NSERC), Canada Graduate Scholarships – Master's program (CGS M) and Fonds de recherche du Québec Nature et technologies (FRQNT) Master Research Scholarship.

Amélioration de la stabilité des bains de support à base de mousse d'albumine à l'aide de pectine pour la bioimpression intégrée

Melanie RODGER

RÉSUMÉ

Les domaines de l'ingénierie tissulaire et de la médecine régénérative visent à restaurer ou à remplacer des tissus et organes endommagés pour le développement de nouvelles thérapies, de modèles de maladies physiologiquement pertinents et, à long terme, d'organes biofabriqués capables de répondre à la pénurie mondiale d'organes destinés à la transplantation. Pour atteindre ces objectifs, des techniques avancées de biofabrication comme la bio-impression 3D intégrée (terme anglais: embedded bioprinting) jouent un rôle central, car elles permettent la création contrôlée de structures cellulaires complexes à haute précision. La bio-impression 3D intégrée permet la création de structures complexes encapsulé avec des cellules vivantes par l'extrusion des bio-encres dans des bains de support. Cette approche a élargi l'éventail des bio-encres imprimables et rendu possible la fabrication de géométries sophistiquées. Toutefois, les matériaux de support actuellement utilisés présentent des limites liées à leur instabilité ainsi qu'à une diffusion insuffisante d'oxygène et de nutriments, ce qui restreint la durée des impressions et compromet la fidélité des structures. Des mousses à base d'albumine ont récemment été proposées comme alternatives perméables à l'oxygène et aux nutriments; cependant, leur dégradation rapide freine leur utilisation à plus grande échelle.

La présente thèse rapporte la stabilisation de mousses d'albumine par l'incorporation de pectine, un polysaccharide biocompatible. Trois formulations — albumine seule (A8), albumine avec 1 % de pectine (A8P1) et albumine avec 2 % de pectine (A8P2) — ont été évaluées en fonction de leur stabilité, de la morphologie des bulles, des propriétés rhéologiques, des caractéristiques physicochimiques et de leur biocompatibilité. L'ajout de pectine a considérablement retardé le drainage et la coalescence des bulles tout en préservant les propriétés rhéologiques essentielles telles que le comportement pseudoplastique (shear-thinning) et la capacité de récupération rapide après déformation. Ces améliorations ont permis l'impression assistée d'hydrogels de chitosane, une bio-encre de faible viscosité et à gélification lente, sous forme de structures multicouches et libres, présentant une grande fidélité. Les experiences de viabilité cellulaire ont par ailleurs confirmé que la pectine ne compromettait pas la biocompatibilité; en particulier, la formulation A8P1 a fourni le microenvironnement le plus favorable et a surpassé les bains de support conventionnels de gélatine lors d'incubations prolongées, en raison d'une meilleure diffusion de l'oxygène et d'un pH plus physiologique. Dans l'ensemble, les mousses albumine–pectine se présentent comme un système de support simple, biocompatible et auto-éliminable, qui surmonte des limitations majeures de l'impression assistée par support et élargit l'éventail des bio-encres imprimables. En facilitant la fabrication fiable de structures cellulaires complexes, cette approche contribue à l'avancement de l'ingénierie tissulaire et de la médecine régénérative, soutenant ainsi le développement futur de modèles de maladies, d'outils de dépistage pharmacologique et, à terme, d'organes bio-imprimés pour répondre à la pénurie d'organes.

Mots-clés: Bioimpression 3D, Bioimpression intégrée, Mousse, Pectine, Albumine

Enhancing the Stability of Albumin Foam-based Support Baths using Pectin for Embedded Bioprinting

Melanie RODGER

ABSTRACT

Tissue engineering and regenerative medicine aim to restore or replace damaged tissues and organs and has key applications in developing advanced therapeutic solutions, physiologically relevant disease models, and engineered tissues that could one day help address the global organ shortage. Achieving these goals requires advanced biofabrication techniques capable of producing complex, cell-laden architectures with high precision and biological relevance—an area where embedded bioprinting has shown great promise. Embedded bioprinting enables the creation of complex, cell-laden structures by extruding bioinks into a support bath that physically supports the printed constructs. This strategy has expanded the range of printable bioinks and has allowed for the fabrication of intricate geometries; however, current support bath materials have several limitations including, insufficient oxygen and nutrient delivery and strenuous support bath removal steps. To combat such limitations, albumin-based foams have recently been proposed as a class of self-removable, oxygen- and nutrient-permeable support bath materials. The main drawback of using foams as a support is that their rapid degradation limits their use for longer, more complex prints.

In this thesis, the stabilization of albumin foams through the incorporation of pectin, a biocompatible polysaccharide is reported. Three formulations—albumin-only (A8), albumin with 1% pectin (A8P1), and albumin with 2% pectin (A8P2)—were evaluated with respect to foam stability, bubble size and distribution, rheological properties, physicochemical properties, printability and biocompatibility. The addition of pectin significantly delayed liquid drainage and bubble coalescence while preserving key rheological characteristics such as shear-thinning and rapid recovery of properties after subjected to deformation. These enhancements supported the embedded printing of chitosan, a low-viscosity and slow-crosslinking hydrogel, into multilayered and freeform constructs with high fidelity. Cell viability assays further confirmed that pectin did not impair biocompatibility; notably, A8P1 provided the most favorable microenvironment and outperformed conventional gelatin-based FRESH baths during extended incubation, owing to enhanced oxygen diffusion and a more physiological pH. Collectively, these findings establish pectin-stabilized albumin foams as a simple, biocompatible, and self-removable support system that addresses key limitations of embedded bioprinting and broadens the range of printable bioinks. By enabling the reliable fabrication of complex, cell-laden constructs, this work contributes to the advancement of tissue engineering and regenerative medicine, supporting future applications in disease modeling, drug testing, and ultimately the development of engineered tissues and organs to combat the organ shortage crisis.

Keywords: 3D bioprinting, Embedded bioprinting, Foam, Pectin, Albumin

PREFACE

The experimental work presented in the following thesis was conducted in the Biomaterials and BioFabrication (BBF) Laboratory at the University of Montreal Hospital Research Centre (CRCHUM). The contents of the thesis are under consideration for publication in a peer-reviewed journal.

Élisabeth Poirier performed the salinity measurements and assisted with the set up and calibration of the device used for the dissolved oxygen measurements. Elise Wasmer performed the SEM imaging and Francesco Touani Kameni performed the histological analysis.

Below are lists of journal articles and conference proceedings published during the author's M.A.Sc. studies in chronological order.

Peer Reviewed Journal Articles

1. **Rodger, M.**, Poirier, É., Wasmer, E., Kameni, F. T., Lerouge, S., Ahmadi, A. (2025). Enhancing the Stability of Albumin Foam-based Support Baths using Pectin for Embedded Bioprinting, *Biomedical Materials* (under review).
2. Wheatley, S. K., Dupeyroux, L., **Rodger, M.**, Hamoud-Michel, H., Lerouge, S., Maurice, C. F., & Ahmadi, A. (2025). Microfluidic Encapsulation of the Human Microbiota – A Tool for Research and Beyond, *Microsystems and Nanoengineering* (under review).
   Contributions: M. Rodger performed the rheological tests and associated analysis

Conference Presentations and Proceedings

1. **Rodger, M.**, Lerouge, S., Ahmadi, A. Enhancing the Stability of Foam-based Support Baths using Pectin for Embedded Bioprinting. The International Conference on Biofabrication 2024, Fukuoka, Japan, November 10–13, 2024.
2. **Rodger, M.**, Lerouge, S., Ahmadi, A. Enhancing the Stability of Foam-based Support Baths using Pectin for Embedded Bioprinting. Concours de vulgarisation ÉTS. Montreal, Canada, February 26, 2025.

3. **Rodger, M.**, Développement d'un support à base de mousse pour la bio-impression 3D des bio-encres. Ma thèse en 3 minutes (itechsanté). Montreal, Canada, March 13, 2025.
4. **Rodger, M.**, Lerouge, S., Ahmadi A. Development of a Pectin-stabilized Albumin-based Foam Support Bath for Embedded Bioprinting. 39th Annual Meeting of the Canadian Biomaterials Society (CBS 2025). Kingston, Canada, May 21-23, 2025.
5. Dupeyroux, L., Wheatley, S. K., **Rodger, M.**, Lerouge, S., Maurice, C. F., Ahmadi, A. Microencapsulation of Intestinal Bacteria: Enhancing Cell Activity via RGD. The Canadian Biomaterials Society Congress (CBS 2025). Kingston, Canada, May 21-23, 2025.
6. **Rodger, M.**, Lerouge, S., Ahmadi, A. Optimizing pectin-stabilized albumin-based foams for enhanced support bath stability in in-foam embedded bioprinting. CSME-CFDSC-CSR 2025. Montreal, Canada, May 25-28, 2025.
7. Dupeyroux, L., Wheatley, S. K., **Rodger, M.**, Lerouge, S., Maurice, C. F., Ahmadi, A. Microencapsulation of intestinal bacteria: Impact of RGD on cell activity. Proceedings of the Canadian Society for Mechanical Engineering International Congress (CSME 2025), Montreal, Canada, May 25-28, 2025.
8. **Rodger, M.**, Lerouge, S., Ahmadi, A. Pectin-Enhanced Albumin Foam for Stable and Biocompatible Support Baths in Embedded Bioprinting. The International Conference on Biofabrication 2025, Warsaw, Poland, September 14–17, 2025.

TABLE OF CONTENTS

LIST OF TABLES

LIST OF FIGURES

LIST OF ABBREVIATIONS

ÉTS	École de Technologie Supérieure
CRCHUM	University of Montreal Hospital Research Center
BBF	Biomaterials and BioFabrication Laboratory
3D	Three-Dimensional
ANOVA	Analysis of Variance
HSD	Honestly Significant Difference
FRESH	Freeform Reversible Embedding of Suspended Hydrogels
GHost	Guest-Host
DMEM	Dulbecco's Modified Eagle Medium
FBS	Fetal Bovine Serum
PBS	Phosphate-Buffered Saline
DPBS	Dulbecco's Phosphate-Buffered Saline
DI	Deionized
A8	8% Albumin
P1	1% Pectin
P2	2% Pectin
SHC	Sodium Hydrogen Carbonate
BGP	β-Glycerophosphate
ECM	Extracellular Matrix

dECM	Decellularized Extracellular Matrix
CAD	Computer-Aided Design
FDM	Fused Deposition Modeling
DMLS	Direct Metal Laser Sintering
EDTA	Ethylenediaminetetraacetic Acid
SDS	Sodium Dodecyl Sulphate
UV	Ultraviolet
GelMA	Gelatin Methacryloyl
PEG	Polyethylene glycol
HA	Hyaluronic Acid
EtOH	Ethanol/Ethyl Alcohol
PDMS	Polydimethylsiloxane
H&M	Hematoxylin and Eosin
SEM	Scanning Electron Microscopy

LIST OF SYMBOLS AND UNITS OF MEASUREMENTS

rpm	revolutions per minute
M	molar
cm	centimeter
mm	millimeter
µm	micrometer
mm/s	millimeter per second
G	gauge
ppt	parts per thousand

INTRODUCTION

The fields of tissue engineering and regenerative medicine aim to restore or replace damaged tissues and organs by combining cells, biomaterials, and bioactive factors to recreate functional biological structures (Hoang *et al.*, 2025). These disciplines are critical for addressing the growing demand for organ transplants, accelerating wound healing, and providing physiologically relevant disease models for drug testing and research. Within this context, three-dimensional (3D) bioprinting has emerged a powerful tool for advancing these fields (Zeng *et al.*, 2022). This technology is capable of fabricating living tissue constructs in a controlled manner by depositing cells and biomaterials (bioinks) within a 3D scaffold (Bao *et al.*, 2020). In recent years, there has been a shift in focus toward developing biofabrication techniques that employ biomaterials capable of accurately mimicking the porous structure and time-dependent viscoelastic properties of native tissues (Zeng *et al.*, 2022; Bao *et al.*, 2020). Enhanced cell viability, proliferation, promotion of differentiation and facilitation of cell migration have all been demonstrated by using bioinks that mimic in vivo properties (Hull *et al.*, 2023; Wu, Jeffreys, Diba & Mooney, 2022; Wei *et al.*, 2020; Chen *et al.*, 2017; Parmar *et al.*, 2016; Courbot & Elosegui-Artola, 2025). However, while biologically relevant bioinks promote favorable cellular responses, they must also exhibit the rheological and mechanical properties required for precise extrusion and shape retention during printing. Soft, low-viscosity materials such as extracellular matrix (ECM)-derived hydrogels and chitosan-based inks often fail to meet these demands, leading to structural collapse, spreading, and poor shape fidelity after deposition (Taghizadeh *et al.*, 2022; Zhang *et al.*, 2023a). Despite significant progress in conventional bioprinting technologies, achieving complex, high-resolution constructs remains a major challenge, particularly for printing freeform or overhanging geometries that require self-supporting materials (Shiwarski, Hudson, Tashman & Feinberg, 2021). As a result, there is an inherent trade-off between biofunctionality and printability which makes it challenging to fabricate intricate, vascularized structures that are essential for the successful creation of functional tissue constructs (Schwab *et al.*, 2020).

Embedded bioprinting is a 3D bioprinting technique that allows for a wide choice of bioinks to be used, including materials that mimic important in vivo properties but lack the required mechanical properties for good printability (Zeng *et al.*, 2022). This is because in embedded bioprinting, bioinks are printed directly into a reservoir containing a supporting matrix, which serves to temporarily maintain the shape of the deposited material during the printing process (Wu *et al.*, 2022). The support bath material must therefore allow the print needle to move through it freely while providing sufficient yield stress to prevent collapse of the printed features, and without damaging the support itself. It must also be possible for the support bath to be easily removed without harming the printed structure as well as to allow for the diffusion of nutrients and gases to the cells being printed (Shiwarski *et al.*, 2021). These demands result in the choice of support bath material to be both a critical and challenging component of this technique. One of the most common methods for embedded bioprinting is Freeform Reversible Embedding of Suspended Hydrogels (FRESH) which uses a slurry of gelatin microparticles as the support (Hinton *et al.*, 2015). Other popular support bath materials to date include gellan gum fluid gels (Compaan, Song & Huang, 2019), carbopol gels (Hinton, Hudson, Pusch, Lee & Feinberg, 2016), agarose slurries (Cidonio *et al.*, 2019), and pluronic blends (Rahimnejad, Adoungotchodo, Demarquette & Lerouge, 2022; Hu *et al.*, 2023). Each of these materials come with their own set of limitations, with lack of oxygenation and poor nutrient delivery to the printed cells over long periods of time and strenuous support bath preparation and removal steps being the most prominent.

One recent technique to overcome these challenges, is in-foam bioprinting, wherein a nutrient enriched albumin-based foam is used as the supporting matrix (Madadian *et al.*, 2024b). By mechanically mixing the protein albumin in cell culture media, a foam capable of performing as a support bath for embedded bioprinting is produced. The key advantages of using foam as the support are that the bubbles permit any cells printed into it to have easy access to oxygen while still having access to nutrients thanks to the cell culture media and since foam is known

to naturally breakdown over time, this allows for a self-removable support. The feasibility of foam as a support has been demonstrated in terms of acceptable rheological properties, good printability and high cell viability. However, the major limitation of albumin-based foam is that it lacks stability and degrades too rapidly, limiting its application for longer prints. Foams are thermodynamically unstable systems causing them to naturally breakdown over time and must therefore be stabilized to be used for more complex embedded bioprinting applications (Linke & Berger, 2011). The addition of polysaccharides such as pectin have been shown in the literature to help stabilize protein-based foams (Zhang *et al.*, 2023b; Miquelim, Lannes & Mezzenga, 2010).

Pectin is a high molecular weight, carboxylated anionic polysaccharide commonly used as a foam stabilizer in the food industry, as it preferentially interacts with the aqueous phase of foams rather than with hydrophobic surfaces such as albumin-coated air bubbles (Schmidt, Novales, Boué & Axelos, 2010). Further, pectin has been used as a biocompatible material in several biomedical engineering applications including wound healing (Amante *et al.*, 2023), drug delivery systems (Méndez *et al.*, 2023), and tissue engineering (Eivazzadeh-Keihan *et al.*, 2022; Morello, De Iaco, Gigli, Polini & Gervaso, 2023). It is hypothesized that adding pectin to albumin-based foam support baths will slow down the liquid drainage, bubble coalescence and disproportionation as a result of favorable interactions within the aqueous phase of the foam such as entanglement of polymer networks and increasing viscosity (Miquelim *et al.*, 2010; Zhang *et al.*, 2023b). In turn, this will permit the foam support to be used for longer and more complex prints, all while maintaining the key advantages of the in-foam bioprinting technique: bubbles providing cells with easy access to oxygen during the printing process and self-removability.

In this thesis, the addition of pectin is used to stabilize albumin-based foam support baths for embedded bioprinting. An 8% w/v albumin foam, henceforth referred to as A8 was compared to foams with varying concentrations of pectin: 8% w/v albumin with 1% pectin (A8P1) and 8%

w/v albumin with 2% w/v pectin (A8P2). The foams were characterized in terms of stability, bubble morphology, rheology, physiochemical properties and biocompatibility. Pectin was successful in slowing the coalescence and liquid drainage of the foams. The albumin-pectin stabilized foams maintained the key rheological properties required in for support baths in embedded bioprinting. Low viscosity, slow crosslinking hydrogels, were successfully printed in the albumin-pectin foams. Cell viability tests using L929 fibroblast cells demonstrated that the addition of pectin did not hinder cell viability, with the A8P1 formulation showing increased viability compared to traditional FRESH techniques over long incubation times. Overall, the results signal that pectin successfully increases foam stability giving in-foam bioprinting a promising future for one day developing more complex functional tissue constructs and help advance the fields of tissue engineering and regenerative medicine.

CHAPTER 1

LITERATURE REVIEW

1.1 Tissue Engineering and Regenerative Medicine

Modern healthcare systems face mounting pressure from an aging population, chronic diseases, and an increasing demand for organ transplants – a demand that far exceeds current supply. In 2020, 107,000 people in the United States alone were on the waiting list for a lifesaving organ transplant, with only approximately 35% of patients receiving a transplant (Tong & Voronov, 2022). In addition, among successful transplants, organ rejection remains a major threat even with immunosuppression (Olson, Atala & Yoo, 2011). Despite advancements in synthetic implants (Mooney & Vacanti, 1993), biomaterials (Li & Kawashita, 2011), and pharmacologic therapies (De Graav *et al.*, 2025), most fall short of replicating the complexity and functionality of native human tissue. As a result, transplantation continues to represent the only viable option for many patients, yet it remains limited by immunological compatibility and donor availability — two obstacles that are difficult to overcome. In response to these limitations, researchers from multiple disciplines began pursuing biological tissue replacement strategies, ultimately leading to the emergence of the field now known as tissue engineering (Olson *et al.*, 2011).

In recent decades, tissue engineering has emerged as a potential solution to the organ shortage problem. Tissue engineering can be described as a multidisciplinary field that combines principles of engineering and biology to integrate cells, biomaterials, and biochemical signals to construct functional biological substitutes (Han *et al.*, 2020; Almouemen, Kelly & O'leary, 2019; Atala & Lanza, 2002). It began to be recognized as a distinct field starting in the late 1980s, with the aim of regenerating tissue made of cells to repair, replace or regenerate damaged or diseased tissue (O'brien, 2011). In 1993, Langer and Vacanti published their landmark paper titled "Tissue Engineering" which helped solidify the shift from aiming to replace damaged tissue with inert materials to regenerating and restoring the function of such tissue using living cells, scaffolds and biological signals (Vacanti & Langer, 1993). Today, tissue engineering can be recognized as a key discipline within the broader field of regenerative medicine with the two terms often being

used interchangeably and can be grouped together as the field tissue engineering and regenerative medicine (TERM) (Hoang *et al.*, 2025). Using tissue engineering and regenerative medicine to regenerating an organ using the patient's own cells would potentially solve the organ shortage and organ transplant rejection issues, revolutionizing modern medicine (Rouchi & Mahdavi-Mazdeh, 2015). Furthermore, as the field has grown and new strategies have been developed, other potential applications beyond fabricating functional tissues and organs have surfaced such as, generating 3D disease models for in vitro drug testing (Armstrong & Stevens, 2019). This can help reduce the need for animal testing by providing powerful platforms for modeling human diseases in vitro under more realistic, controllable conditions (Vacanti & Langer, 1999; Huh, Hamilton & Ingber, 2011).

Many tissue engineering strategies have been developed to achieve such desired functional tissue substitutes. One of the earliest and most widely studied methods are scaffold-based approaches which use biocompatible and often biodegradable materials to provide seeded cells with structural support (Vacanti & Langer, 1993). Common materials used for the scaffolds include but are not limited to alginate, collagen, chitosan and hyaluronic acid (HA) (Eltom, Zhong & Muhammad, 2019). Another popular set tissue engineering strategies is known as cell-based methods. These can include cell sheets, spheroids, and organoids, which work off the principle that cells possess the ability to self-assemble into tissue like structures (Kobayashi, Kikuchi, Aoyagi & Okano, 2019; Lancaster & Knoblich, 2014). This approach is particularly helpful in creating in vitro disease models which are helpful in drug screening and research. Further, the use of decellularized extracellular matrices (dECM) have become another major tissue engineering technique. In this approach, tissue is stripped of all cells and genetic material by one of several existing methods such as using detergents (Roosens *et al.*, 2016), osmotic shock (Poornejad *et al.*, 2016), and super critical CO2 (Guler, Aslan, Hosseinian & Aydin, 2017). When the cells are removed it leaves behind the native ECM and vasculature, offering a biocompatible structural support with the appropriate biochemical cues for recellularization (Kim, Majid, Melchiorri & Mikos, 2019; Badylak, Taylor & Uygun, 2011; Ott *et al.*, 2008; Kort-Mascort *et al.*, 2023).

As tissue engineering has grown, hybrid approaches combining scaffolds, cells and bioactive signals have been developed. Examples of such approaches include microfluidics (Chung, Lee, Khademhosseini & Lee, 2012), electrospinning (Sill & Von Recum, 2008) and three dimensional (3D) bioprinting (Saini *et al.*, 2021). 3D bioprinting harnesses the strengths of multiple tissue engineering strategies and has demonstrated key advantages over conventional techniques (Bishop *et al.*, 2017). 3D bioprinting is a form of additive manufacturing that allows for the precise deposition of cells and biomaterials permitting for high control over the structure of the tissue and heterogeneity (Murphy & Atala, 2014; Mandrycky, Wang, Kim & Kim, 2016). As such, it enables the fabrication of intricate structures with high spatial control that are unattainable with other conventional tissue engineering techniques such as scaffolding (Karamchand *et al.*, 2023). This capability addresses some of the key limitations experienced with earlier tissue engineering methods such as reproducibility and scalability all while opening the door to fabricate complex patient-specific constructs that can have detailed vasculature with multiple cell types. As a result, 3D bioprinting has become one of the leading biofabrcation techniques in the pursuit of creating functional tissue constructs (Ozbolat & Hospodiuk, 2016; Karamchand *et al.*, 2023; Choudhury, Anand & Naing, 2018).

1.2 3D Bioprinting

Three-dimensional (3D) bioprinting is a powerful tool used in tissue engineering and regenerative medicine. Using a digital computer-aided design (CAD) file as a blueprint, this additive manufacturing technology is capable of fabricating living tissue constructs in a controlled manner by depositing cells and biomaterials (bioinks) layer-by-layer to form 3D structures (Zeng *et al.*, 2022; Bao *et al.*, 2020). There exists several different types of 3D bioprinting technologies as well as many different materials that can be printed. In contrast to common additive manufacturing methods such as fused deposition modeling (FDM), binder jetting, and direct metal laser sintering (DMLS) - used to print plastics, ceramics, and metals, respectively - 3D bioprinting instead utilizes soft bioinks, typically hydrogels encapsulating living cells.

1.2.1 Hydrogels used in Bioinks for 3D Bioprinting

Hydrogels are one of the most common biomaterials used in 3D bioprinting and are typically used to form the bioinks to be printed because they mimic in vivo properties by closely resembling the ECM of natural tissues (Xia & Chen, 2022). Hydrogels are composed of natural or synthetic polymers that can form 3D networks and absorb water providing cells with a hydrated, 3D environment with tunable mechanical and biochemical properties (Karoyo & Wilson, 2021). Natural polymers provide a biologically relevant microenvironment that supports cell survival by offering high biocompatibility, natural ligands for attachment and proliferation, and properties that closely mimic the native ECM (Cao, Duan, Zhang, Cao & Zhang, 2021). However, they often lack the mechanical properties necessary for good printability and can experience fast and uncontrolled degradation. Synthetic polymers can help enhance the mechanical properties as they can possess tunable mechanical and chemical properties but are often prepared using toxic reagents which can hinder their biocompatibility. As a result, 3D bioprinting requires a fine balance between high cell viability and acceptable mechanical properties. Although, natural and synthetic hydrogels (hybrid hydrogels) can be used to help find a good balance between biocompatibility and mechanical strength, the tradeoff between good mechanical properties versus good biocompatibility continues to be ongoing challenge faced by this technology (Khoeini *et al.*, 2021; Kačarević *et al.*, 2018).

Another important characteristic of the materials making up the bioinks used in 3D bioprinting is that they undergo a sol-gel-phase transition to form a gel network. To form the hydrogel, a biological precursor undergoes a sol-gel-phase change known as crosslinking or gelation to form the hydrogel itself. Bioinks must be crosslinked either during or after the printing to allow the printed construct to maintain its intended shape and to provide it with structural integrity and to prevent deformation from its own weight (Gungor-Ozkerim, Inci, Zhang, Khademhosseini & Dokmeci, 2018). The gelation or crosslinking mechanism of a hydrogel is dependent on type of material used (Mancha Sánchez *et al.*, 2020). Polymers such as gelatin, agarose and chitosan form a hydrogel through thermal crosslinking where the sol-gel-phase change occurs once a certain transition temperature is reached (Wang *et al.*, 2017; Gong,

Kong & Wang, 2021; Taghizadeh *et al.*, 2022). Ionically crosslinkable materials such as alginate can gel in the presence of divalent cations through the formation of ionic bridges between adjacent polymer chains (Axpe & Oyen, 2016; Grant, Morris, Rees, Smith & Thom, 1973). Photocrosslinkable polymers, including gelatin methacryloyl (GelMA) and HA methacrylate, solidify when exposed to light in the presence of photoinitators. Other crosslinking mechanisms include the use of enzymes to promote the formation of covalent bonds between polymers such as fibrin (de Melo *et al.*, 2020), and by pH fluctuations as used in the crosslinking of collagen (Osidak, Kozhukhov, Osidak & Domogatsky, 2020).

1.2.2 3D Bioprinting Techniques

There are many types of 3D bioprinting techniques depending on the materials used and the intended application. The many 3D bioprinting modalities can be generally separated into two main categories: physical/nozzle based and light based (Figure 1.1). Extrusion-based bioprinting, a physical/nozzle based method, is one of the most widely used 3D bioprinting techniques (Betancourt & Chen, 2022). In this technique, the bioink is extruded out of a print nozzle/needle pneumatically via air pressure or mechanically via vertical and rotational mechanical forces from a piston or a screw, respectively (Derakhshanfar *et al.*, 2018). Extrusion printing, in its broadest definition, can process materials with viscosities ranging from 30 mPa·s to >6 × 10^7 mPa·s, encompassing both soft hydrogels used in bioprinting and highly viscous polymer melts used in thermoplastic extrusion. It is important to note, however, that the practical viscosity range for bioprinting is lower, as excessively high viscosities generate high shear stress during the extrusion process which can compromise cell viability. On the other hand, the use of bioinks with very low viscosites results in poor printability, making it impossible to print highly detailed, complex, hollow, and free-standing constructs (Ravanbakhsh *et al.*, 2021). As such, several techniques have been developed to help address this limitation including coaxial and embedded bioprinting. In coaxial bioprinting, a concentric multiple layered nozzle is used to extrude more than one material at once and can be used to print hollow fibers (Kjar, McFarland, Mecham, Harward & Huang, 2021; Badr, Madadian, MacDonald, Tasker & Ahmadi, 2023). In

emedded bioprinting, the bioink is printed into a support bath to help maintain its shape (Hinton *et al.*, 2015). Embedded bioprinting will be discussed in depth in section 1.3.

Another nozzle-based 3D bioprinting technique is inkjet or droplet-based 3D bioprinting. The droplets can be generated through several techniques with thermal and piezoelectric approaches being the most common (Kumar, Ebbens & Zhao, 2021b). In thermal inkjet bioprinting, an actuator locally heats the bioink which causes vapor bubbles, leading to the ejection of the bioink droplets (Cui, Boland, DD'Lima & K. Lotz, 2012). In piezoelectric inkjet bioprinting, a piezoelectric actuator converts electrical signals into mechanical deformation resulting in volumetric changes in the nozzle which ejects the droplets out (Park, Lee & Jung, 2023). In comparison to extrusion-based, droplet-based bioprinting offers higher resolution, however, it is limited to lower viscosity bioinks due to higher viscosity bioinks causing nozzle cloggage (Li *et al.*, 2020).

Light-based bioprinting is a nozzle-free approach that uses the energy from light to produce 3D constructs (Dou *et al.*, 2021). Compared to physical bioprinting methods, light based methods have very high spatial control, permitting for high printing accuracy and resolution up to the micron level (Chang & Sun, 2023). Laser-induced forward transfer is one type of light based bioprinting where a beam of light is focused through a transparent substrate onto an energy absorbing film made of metal or a polymer (Delaporte & Alloncle, 2016). The film absorbs the light, converting it to internal energy which increases the temperature causing expansion, deformation, and vaporization which results in the transfer of material of a biological solution coating layer beneath the energy absorbing layer (Figure 1.1). However, these types of systems are limited by their high equipment cost and potential thermal or photothermal stress to biological materials (Budharaju, Sundaramurthi & Sethuraman, 2024; Agarwal, Srinivasan, Lather, Pandita & Vasanthan, 2023). Another technique that uses a laser is stereolithography or vat-polymerization 3D bioprinting, where a controlled laser beam cures a liquid photocrosslinkable bioink inside a vat/container (Li *et al.*, 2023). Upon curing the first layer of bioink, the printing platform is moved away from the printing position and fresh liquid bioink for photocuring of the second layer can be exposed to the laser. This series

of steps continues until the desired 3D construct is formed. Despite its excellent resolution, stereolithography is constrained by the need for photocrosslinkable and optically transparent bioinks, limited penetration depth of light, and risks of phototoxicity during crosslinking (Lai *et al.*, 2024; Agarwal *et al.*, 2023).

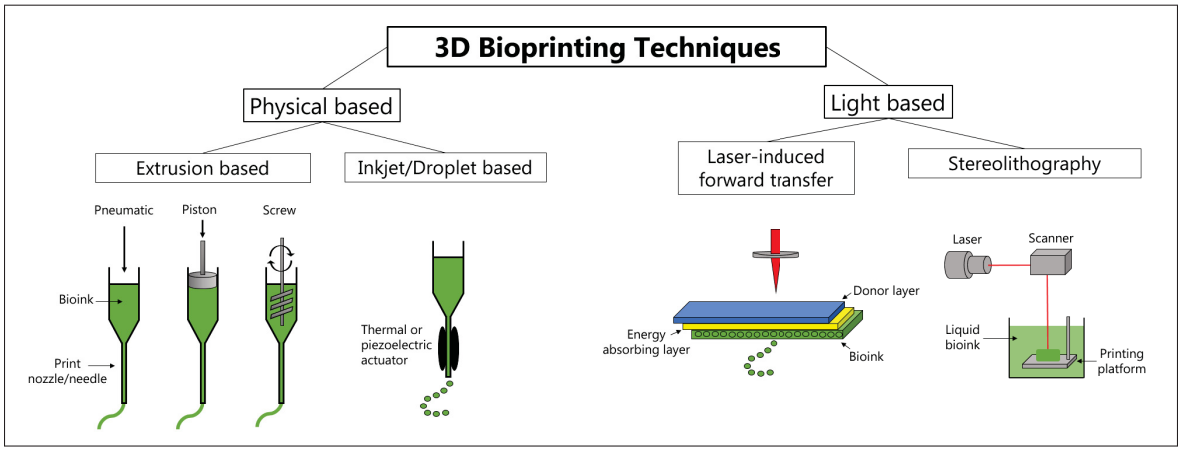

Figure 1.1 Overview of existing 3D bioprinting techniques

1.3 Embedded Bioprinting

Embedded bioprinting is an extrusion-based 3D bioprinting technique wherein bioink is printed directly into a secondary support bath material. The support bath physically supports the bioink being printed, allowing it to crosslink after which the support is removed leaving behind the intended structure. The support bath helps overcome gravitational limits experienced with regular extrusion bioprinting permitting for the development of complex structures with overhanging features with micron resolution (Budharaju *et al.*, 2024). Another advantages of this technique are that it is compatible with a wide range of bioinks. This bioink versatility allows for mechanically weak, low viscosity and slow crosslinking gels which would exhibit poor printability with conventional 3D bioprinting techniques to be printed with excellent shape fidelity (Fang *et al.*, 2023; Cooke, Riffe, Gomes, Domingues & Burdick, 2025; Budharaju *et al.*, 2024; Shiwarski *et al.*, 2021; Madadian *et al.*, 2024b). Embedded bioprinting works because, as the print needle moves through the yield-stress support bath, the bath itself locally liquefies due to the disruption of reversible non-covalent bonds within its structure. Once the needle passes

and the shear forces are removed, these bonds re-form, enabling the support bath to solidify again and securely hold the extruded bioink in its intended shape (Jin, Chai & Huang, 2017; Budharaju *et al.*, 2024). The support bath can be removed following the printing process, leaving behind the printed structure in the desired shape.

Further, there are embedded bioprinting approaches where a sacrificial ink is printed into a functional bioink support bath. In this case, the bioink support bath is solidified and the extruded ink is removed leaving behind channels (Compaan, Song, Chai & Huang, 2020; Skylar-Scott *et al.*, 2019). Such approaches will be touched on in this section, however, the main focus will be to review embedded bioprinting approaches where a bioink is printed into a sacrificial support bath.

1.3.1 Gel-in-Gel Embedded Bioprinting

Embedded bioprinting is commonly described as a gel-in-gel printing technique since a hydrogel bioink is printed into a support bath that is typically composed of a secondary gel in the form of a bulk hydrogel or a slurry of hydrogel microparticles (Ribezzi *et al.*, 2023; Basu, Saha, Goodman, Shafranek & Nelson, 2017; Budharaju *et al.*, 2024). The choice of material used for the support is a critical component of this technique since it must provide cells with a biocompatible environment all while being capable of physically supporting the printed constructs, allow the printer nozzle to move through it freely, and subsequently be removed without damaging the printed structure (Hua *et al.*, 2021). Embedded bioprinting is derived from embedded 3D printing where viscoelastic inks are extruded through nozzles embedded into an elastomeric reservoir in a technique initially used to fabricate strain sensors and software robots (Budharaju *et al.*, 2024). As an extension of this technology, the biomedical engineering field began to substitute the conventional materials used for inks and reservoirs in this method with cell-laden bioinks and biocompatible support baths.

Initial examples of using embedded 3D printing for biological applications can be traced back to 2011 where Wu, DeConinck & Lewis (2011), used an embedded printing technique called

omnidirectional printing to create microvascular networks. Omnidirectional printing works by printing patterns of fugitive inks constructed into thermal or photocurable hydrogel reservoir (Wu *et al.*, 2011). After printing, the reservoir is photopolymerized and the printed ink is liquefied, leaving behind an interconnected microvascular network. Four years later, in 2015, embedded bioprinting saw revolutionary advancements in with three key papers published which focused on sacrificial support bath development: Hinton *et al.* (2015) which introduced Freeform Reversible Embedding of Suspended Hydrogels (FRESH), Bhattacharjee *et al.* (2015) who introduced the writing in the granular gel medium embedded bioprinting technique, and Highley, Rodell & Burdick (2015) which introduced printing into self-healing bulk hydrogels.

1.3.1.1 FRESH

In FRESH embedded bioprinting, the support bath is made of a gelatin microparticle slurry with microparticles that behaves as a yield stress fluid (Hinton *et al.*, 2015; Budharaju *et al.*, 2024). The gelatin microparticles are prepared by mechanically blending a gelatin gel in a method now termed FRESH v1.0. In 2019, FRESH v2.0 was developed where a coacervation process is used instead to generate the microparticles resulting in microparticles with more uniform spherical morphologies, smaller diameter, reduced polydispersity and a tunable storage modulus and yield stress (Lee *et al.*, 2019). These properties permit for higher print resolution. In FRESH, the printed constructs are removed from the gelatin microparticle support bath by increasing the temperature to 37°C, which causes the support to liquefy, leaving behind the printed bioink in its intended structure (Hinton *et al.*, 2015). This technique is compatible with many low viscosity inks that need physical support upon being printed (see Table 1.1). As a result, depending on the type bioink being printed, the gelatin microparticles can be prepared using varying solutions. For instance, the gelatin support bath can be prepared by dissolving gelatin into $CaCl_2$ or $CaSO_4$ solutions to allow for the crosslinking of bioinks that crosslink in the presence of divalent cations (Hinton *et al.*, 2015; Bordoni *et al.*, 2020). The microparticle slurry can also be prepared using cell culture media or a buffer (e.g. PBS 1X or HEPES) (Allevi, 2020). FRESH is widely considered as one of the most popular embedded bioprinting techniques and has been used in

several applications including developing cardiac ventrical models (Lee *et al.*, 2019), heart valve scaffolds (Maxson *et al.*, 2019), and muscle constructs (Choi *et al.*, 2019).

1.3.1.2 Writing in the Granular Gel Medium

Writing in the granular gel medium is an embedded bioprinting technique where bioinks are printed into jammed suspensions of hydrogel microparticles typically of Carbopol or other granular gels that exhibit Bingham plastic behavior (Bhattacharjee *et al.*, 2015). The constructs are subsequently liberated by dilution or washing of the microgel bath. In contrast to FRESH, which relies on gelatin microparticles that can be melted away at physiological temperature, granular gel media are generally synthetic and not inherently biocompatible, requiring careful removal before downstream culture. This distinction highlights how writing in the granular gel medium emphasizes tunable rheology and structural support, while FRESH emphasizes gentle, thermoreversible removal and cell compatibility (Hinton *et al.*, 2015; Bhattacharjee *et al.*, 2015; Brunel, Hull & Heilshorn, 2022). The writing in the granular gel medium technique has been successful in developing complex multiscale structures (Shapira, Noor, Asulin & Dvir, 2018).

1.3.1.3 Self Healing Hydrogels or GHost Embedded Bioprinting

Printing into self healing hydrogels, also termed Guest–host (GHost) embedded bioprinting, exploits supramolecular host–guest interactions to create a self-healing support matrix (Highley *et al.*, 2015; Daly, Davidson & Burdick, 2021). In contrast to the supports used in FRESH and writing in the granular gel medium, this approach uses a bulk hydrogel support bath as opposed to a microparticle suspension. In this technique, the support consists of a HA hydrogel functionalized with β-cyclodextrin (host) and adamantane (guest) moieties, which form reversible inclusion complexes. The resulting network is shear-thinning, allowing a printing nozzle to move smoothly through the bulk gel, and rapidly self-heals after the removal of shear forces to stabilize deposited bioinks in freeform 3D patterns (Shiwarski *et al.*, 2021; Highley *et al.*, 2015; Budharaju *et al.*, 2024). The guest–host hydrogel itself acts as the embedding medium, offering tunable viscoelasticity and recovery dynamics through adjusting the ratio of

the host to guest components. Self healing hydrogels have been used in creating perfusable microchannel networks as well as bioprinting low viscosity photopolymerizable blood-based bioinks (Song, Highley, Rouff & Burdick, 2018; Caiado Decarli *et al.*, 2025).

1.3.1.4 Other Gel-in-Gel Techniques

As embedded bioprinting has grown, additional techniques have been developed, incorporating new materials. A summary of the different support baths used in embedded bioprinting is presented in Table 1.1. The table also includes examples of bioinks compatible with each technique that have been seen in the literature, as well as the removal mechanism required.

1.3.2 Limitations of Gel-in-Gel Embedded Bioprinting

While gel-in-gel embedded bioprinting has expanded the range of printable bioinks, the technique still faces several key limitations. Firstly, some support baths require strenuous and time-consuming preparation and removal steps. For instance: gelatin microparticle baths (e.g. FRESH) require heating to 37°C to induce melting, granular gels such as Carbopol are removed by dilution and washing steps, guest–host hydrogels rely on reversible supramolecular interactions, and alginate-based supports may require chelation with ethylenediaminetetraacetic acid (EDTA) or pH adjustment for clearance (Hinton *et al.*, 2015; Bhattacharjee *et al.*, 2015; Highley *et al.*, 2015). These processes can leave behind residues or expose constructs to harsh chemical or mechanical stresses, risking damage or reduced cell viability. Another important drawback is the limited nutrient and oxygen transport within dense gel support baths, which can compromise long-duration prints or thick constructs (Shiwarski *et al.*, 2021). Finally, some support materials (e.g., nanoclays) are not inherently biocompatible and must be fully removed before long-term culture, adding additional handling steps and sources of variability (Brunel *et al.*, 2022). Together, these limitations highlight the need for more user-friendly, biocompatible, and easily removable support baths to broaden the applicability of embedded bioprinting in tissue engineering.

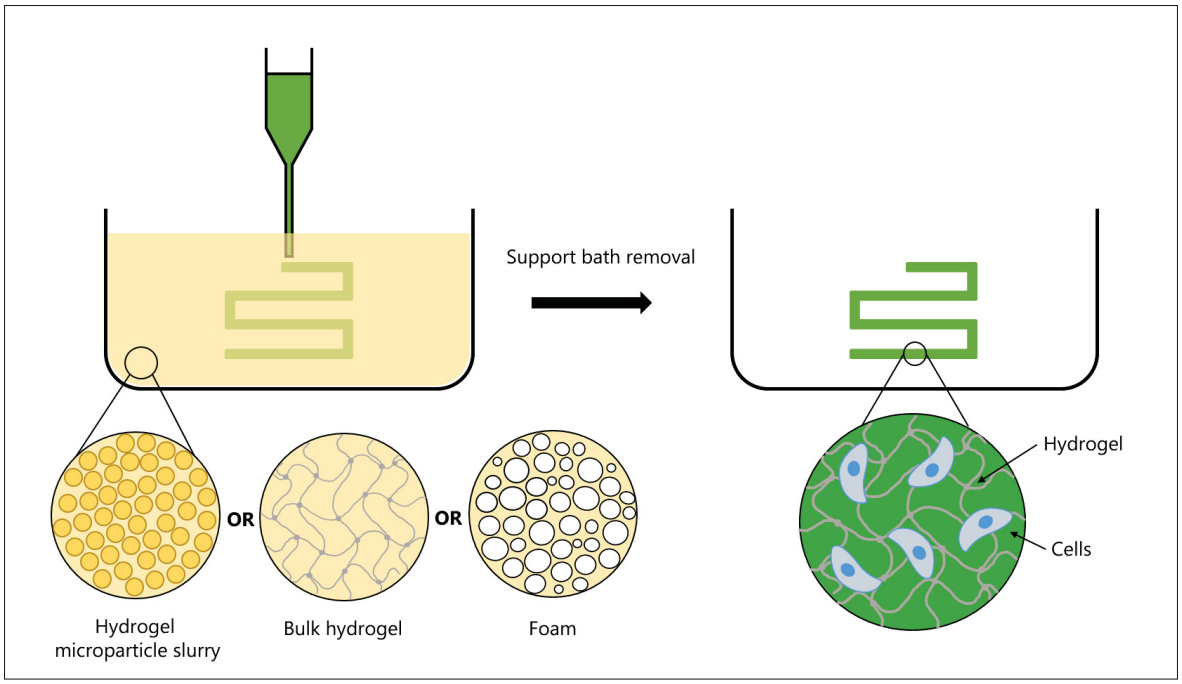

Figure 1.2 Schematic of embedded bioprinting and the type of support bath materials used

1.3.3 In-Foam Bioprinting

Madadian *et al.* (2024b) introduced a novel embedded bioprinting modality termed in-foam bioprinting, which uses an aqueous foam as the support bath as opposed to a gel. In particular, this approach uses a nutrient enriched albumin-based foam as the support bath material. The foam is prepared by dissolving a foaming agent, albumin powder, in cell culture media and is then mechanically foamed, creating bubbles. The mechanical mixing of the albumin causes it to denature, exposing it's hydrophobic and hydrophilic groups which traps the air phase thus forming bubbles (Gharbi & Labbafi, 2019; Duan *et al.*, 2018). In addition to its foaming properties, albumin has been previously used as a biocompatible and biodegradable material (Bajpai & Saini, 2006). The albumin-based foam was successfully used as a support bath exhibiting the appropriate rheological properties, the ability to print freeform structures and overhanging structures with acceptable printability (Taghizadeh *et al.*, 2022). The foam support was easily removed after printing, as the liquid phase of the foam naturally drained downward

due to its higher density while the bubbles gradually coalesced as the foam naturally broke down. To ensure complete removal, negative pressure was also applied to clear any residual foam from the constructs.

The inspiration behind using foam as a support is that it may address some of the limitations faced with current traditional gel-based support baths outlined in section 1.3.2 such as lack of oxygenation and complications with bath removal (Madadian *et al.*, 2024b). Since foam is made out of bubbles, it is possible that it would allow the printed constructs to have easier access to oxygen and since the aqueous phase of the foam is cell culture media there is also nutrient availability. This has yet to be investigated in depth. Secondly, since foams naturally breakdown over time it leads to their removal after the printing process to be more straightforward. The main drawback of in-foam bioprinting lies in the instability of albumin foam. Since the bubbles coalesce and liquid drains rapidly, the foam breaks down quickly and provides only a limited window for printing. This short lifespan constraints the technique to relatively simple or short-duration prints, making it unsuitable for fabricating larger or more complex constructs. To advance toward practical use, particularly in tissue engineering where long print times and construct fidelity are essential, more stable foam formulations will be required.

Table 1.1 Summary of support bath materials used in the literature as well as compatible bioinks used for each support in the literature and the respective support bath material removal mechanism

Support Bath Material	**Compatible Bioinks**	**Removal Mechanism**	**Refs.**
Gelatin microparticles	• low viscosity hydrogels • alginate • alginate-HA composite hydrogels • fibrinogen-HA-albumin • collagen • collagen-matrigel-firbinogen-HA • MeHA • GelMA	Liquification at 37°C	(Hinton *et al.*, 2015; Brunel *et al.*, 2024; Budharaju *et al.*, 2024; Shapira *et al.*, 2018; Budharaju *et al.*, 2024; Catori *et al.*, 2022)
Carbopol	• GelMA • collagen • alginate • polydimethyl-siloxane (PDMS)	Dilution and washing with Dulbecco's PBS (DPBS), aspiration of the support bath	(Villata *et al.*, 2024; Ning *et al.*, 2020; Brunel *et al.*, 2024; Jin, Compaan, Bhattacharjee & Huang, 2016; Hinton *et al.*, 2016)

Support Bath Material	**Compatible Bioinks**	**Removal Mechanism**	**Refs.**
HA modified with adamantane and β-cyclodextrin	• guest-host HA hydrogel • alginate • mesenchymal stem cell and cardiac spheroids	Dilution with buffer, gentle aspiration	(Highley *et al.*, 2015; Daly *et al.*, 2021)
Nanoclays (laponite)	• alginate • alginate-gelatin composite hydrogels • hydrogel with enough mechanical strength to be physically removed from support bath	Dilution, washing with NaCl, removing printed construct itself from the support bath	(Jin *et al.*, 2021; Afghah, Altunbek, Dikyol & Koc, 2020)

Support Bath Material	**Compatible Bioinks**	**Removal Mechanism**	**Refs.**
Pluronic blends	• collagen • chitosan • chitosan-gelatin composite hydrogels • alginate • GelMA • PEG-based hydrogels	Liquefaction at lower temperature (4°C), dilution	(Brunel *et al.*, 2024; Rahimnejad *et al.*, 2022; Rocca, Fragasso, Liu, Heinrich & Zhang, 2018; Wang *et al.*, 2025; Zhang *et al.*, 2024)
Agarose microgels	• GelMA • alginate • alginate-gelatin composite hydrogels • alginate-collagen composite hydrogels	Dilution of slurry with cell media	(Yang, Liu, Gao, Zhang & Wu, 2022; Mirdamadi, Muselimyan, Koti, Asfour & Sarvazyan, 2019)
Alginate microgels	• cell-only bioink	Washing	(Jeon *et al.*, 2019)

Support Bath Material	**Compatible Bioinks**	**Removal Mechanism**	**Refs.**
Calcium-alginate nanoparticles - xanthan gum hybrid support bath	• collagen	Enzymatic reaction with alginate lyase at 37° or chleation-mediated dissolution	(Shapira, Noor, Oved & Dvir, 2020)
Gellan gum microparticles	• gelatin • alginate • PEGDA • bioinks that crosslink via physical, enzymatic and photocrosslinking mechanisms	Agitation in PBS	(Brunel *et al.*, 2022; Compaan *et al.*, 2019)
Xanthan gum - gelatin composite support bath	• alginate • GelMA	Dilution with buffer and aspiration of the support	(Lai & Meagher, 2024)
Albumin-based foam	• low viscosity, slow crosslinking hydrogels such as chitosan	self-removable with natural breakdown of foam, aspiration of any remaining foam	(Madadian *et al.*, 2024b)

1.4 Methods to Stabilize Aqueous Foams

Foams are thermodynamically unstable systems with a thin viscoelastic film surrounding the air, known as the lamella, experiencing stabilization and destabilization forces (Linke & Berger, 2011). The mechanism behind destabilization of aqueous foams can be described by three simultaneous phenomena: bubble coalescence, liquid drainage, and disproportionation (see Figure 1.3) (Zhan, Youssef, Shah, Li & Li, 2022). Bubble coalescence describes the merging of bubbles. Liquid drainage is the process of the aqueous phase of the foam flowing out of the foam structure; it is driven by gravity and capillary forces that act on the liquid films separating the bubbles resulting in the foam shrinking. Disproportionation is the diffusion of gas molecules from small to large bubbles driven by pressure differences (Pitois, 2012). Although these three phenomena are inevitable in aqueous foams, there exists several techniques to delay and slow down their occurrence including, surfactant stabilization, polysaccharides stabilizers, and particle-based (Pickering) stabilization.

1.4.1 Surfactant Stabilization

Surfactants, also termed surface active agents, are amphiphilic compounds containing at least one lyophilic/hydrophilic group and one lyophobic/hydrophobic group (Karsa & Houston, 2006). They reduce the surface tension of a liquid by migrating to the gas/liquid interfaces and orientating themselves to minimize the contact between hydrophobic groups and the liquid phase. As a result, surfactants can act as foaming agents by assembling at the air–liquid interface, where their hydrophobic regions orient toward the air phase inside the bubbles, while the hydrophilic regions interact with the surrounding aqueous phase. A common example of a surfactant is sodium dodecyl sulphate (SDS) which can be found in foaming personal care products such as shampoo. However, SDS is cytotoxic and in the context of using a foam for embedded bioprinting, more biocompatible foaming agents are required (Arenholt-Bindslev, Bleeg & Richards, 1992). For instance, proteins such as albumin and casein can act as natural, macromolecular surfactants, adsorbing at the air-liquid interface to lower surface tension and

form bubbles with viscoelastic films that resist immediate coalescence (Damodaran, 2005; Abeyrathne, Lee & Ahn, 2013; Ince Coşkun & Özdestan Ocak, 2021).

1.4.2 Polysaccharide Stabilizers

Polysaccharides can be added to foam systems to help enhance their stability (Miquelim *et al.*, 2010). Although surfactants and proteins can behave as foaming agents, creating a network of bubbles, in many cases the foam is not stable for long periods of time. Polysaccharides can be added to such foams as stabilizers to help delay their breakdown by increasing the bulk viscosity, slowing liquid drainage, and forming viscoelastic networks in the aqueous phase (Murray, 2007; Dickinson, 2010). The combination of proteins and polysaccharides has a synergistic effect on the surface activity of the bubbles with the proteins anchoring the air phase and hydrophilic polysaccharides anchoring the aqueous phase contributing electrostatic repulsion and steric hindrance (Zhan *et al.*, 2022; Bouyer, Mekhloufi, Rosilio, Grossiord & Agnely, 2012). Common examples include pectin, xanthan gum, guar gum, κ-carrageenan, and cellulose derivatives (Zhan *et al.*, 2022; Han, Zhu, Zhang & Liu, 2024) . For instance, pectin, a polysaccharide derived from citrus peel, has been commonly used in the food industry as a thickener, gelling agent and foam stabilizer (Toniazzo & Fabi, 2023). It has been used to successfully stabilize both albumin and napin protein-based proteins extending the lifetime of the foams (Sadahira *et al.*, 2015; Schmidt *et al.*, 2010). Further, pea and faba bean protein foams have been found to be stable only upon the addition of the polysaccharide xanthan gum (Mohanan, Nickerson & Ghosh, 2020). Polysaccharide additives are particularly attractive for biomedical and food applications due to their biocompatibility, renewability, and ability to produce foams with controllable stability and viscosity (Murray, 2007; Zhang *et al.*, 2023b).

1.4.3 Particle-Based (Pickering) Stabilization

Pickering foams are stabilized by the adsorption of small solid particles to the air-liquid interface forming a rigid shell around bubbles physically preventing coalescence of the bubbles (Lam, Velikov & Velev, 2014). The stabilization occurs through mechanical reinforcement as opposed

to surfactant adsoprtion. Commonly used materials include silica nanoparticles, cellulose nanocrystals, and starch granules (Lam *et al.*, 2014). While Pickering systems produce highly stable foams with resistance to coalescence and drainage, they have yet to be used as a support bath in embedded bioprinting. They may present potential limitations since the adsorbed particles are often irreversibly attached to bubble surfaces, which could introduce difficulties in removing the foam cleanly after printing. Moreover, cytocompatibility concerns, and limited self-healing behavior may also hinder their performance as support baths; however, future work beyond the scope of this thesis would be required to properly investigate the suitability of Pickering foams in this context (Brown, de la Pena & Razavi, 2023).

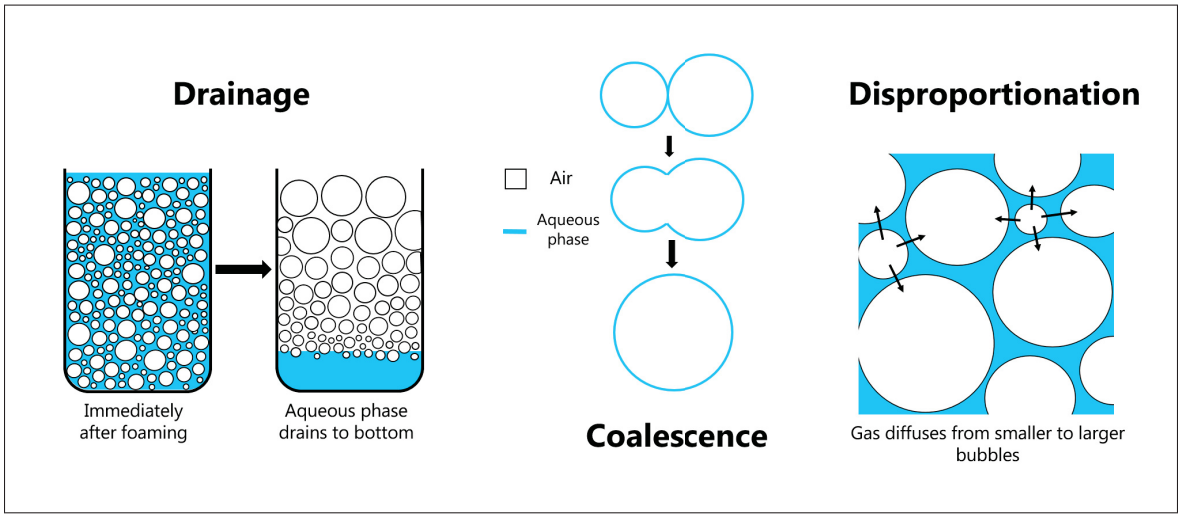

Figure 1.3 Schematic of the different mechanisms that drive the destabilization and breakdown of aqueous foams

1.5 Knowledge gap

Although there have been considerable advancements in tissue engineering and 3D bioprinting, there still exists critical limitations that prevent it from attaining its full potential in addressing the organ shortage and other key applications (e.g. advanced disease models). Although gel-in-gel embedded bioprinting has helped propel the field forward by permitting for more complex structures to be printed, this technique has several drawbacks. In-foam bioprinting has the potential to overcome some of these limitations, however, the albumin-based foam lacks the

stability required to be used for longer prints. Polysacccharide stabilizers have been shown to stabilize albumin-based foams and foams in general. Although there is strong evidence that the addition of polysaccharides to foams increase their stability, it has yet to be explored in the context of stabilized foam-based support baths for embedded bioprinting.

1.6 Hypothesis

It is hypothesized that the addition of a polysaccharide to a protein-based foam will enhance its stability and make it more suitable as a support bath for embedded bioprinting.

1.7 Research Objectives

The work presented in this thesis is guided by the objectives outlined below:

Objective 1: Identify an appropriate stabilizer for foam-based support for embedded bioprinting.

Objective 2: Examine the impact of the stabilizer on the stability, foaming, and viscoelastic properties of the foam.

Objective 3: Examine the impact of the stabilizer on printability and cell viability within the foam.

CHAPTER 2

ENHANCING THE STABILITY OF ALBUMIN FOAM-BASED SUPPORT BATHS USING PECTIN FOR EMBEDDED BIOPRINTING

M. Rodger[1,2], É. Poirier[1,2], E. Wasmer[2], F. T. Kameni[2], S. Lerouge[1,2,3,*], A. Ahmadi[1,2,*]

[1] Department of Mechanical Engineering, École de technologie supérieure,
1100 Notre-Dame St W, Montreal, Quebec, Canada H3C 1K3
[2] Biomaterials and BioFabrication Laboratory (BBF), University of Montreal Hospital Research Center (CRCHUM),
900 Saint Denis St, Montreal, Quebec, Canada H2X 0A9
[3] Department of Pharmacology and Physiology, Université de Montréal,
2900 Edouard Montpetit Blvd, Montreal, Quebec, Canada H3T 1J4

[*] Correspondence: sophie.lerouge@etsmtl.ca; ali.ahmadi@etsmtl.ca

Paper submitted for publication in *Biomedical Materials*, August 2025

2.1 Abstract

Embedded bioprinting enables the fabrication of complex, cell-laden structures by extruding bioinks into support baths. This technique has advanced the field of tissue engineering by expanding the range of printable bioinks and enabling the creation of intricate geometries; however, limitations such as instability and inadequate oxygen and nutrient delivery in current support materials restrict long print durations and compromise fidelity. Recently, albumin-based foams have been proposed as oxygen- and nutrient-permeable supports, but their rapid degradation restricts practical use. Here, we report the stabilization of albumin foams through the incorporation of pectin, a biocompatible polysaccharide. Three formulations—albumin-only (A8), albumin with 1% pectin (A8P1), and albumin with 2% pectin (A8P2)—were evaluated for foam stability, bubble morphology, rheology, and physicochemical properties. Pectin significantly delayed drainage and bubble coalescence while maintaining essential rheological features such as shear-thinning and recovery. These improvements enabled the embedded printing of chitosan, a low-viscosity and slow-crosslinking hydrogel, into multilayered and freeform structures with high fidelity. Cell viability assays confirmed that pectin did not compromise biocompatibility; A8P1 provided the most favorable microenvironment and outperformed conventional FRESH

baths during extended incubation, owing to enhanced oxygen diffusion and a more physiological pH. Overall, pectin-stabilized albumin foams offer a simple, biocompatible, and self-removable support system that addresses key limitations of embedded bioprinting and broadens the range of printable bioinks.

2.2 Introduction

Three-dimensional (3D) bioprinting has emerged as a transformative tool in tissue engineering and regenerative medicine, enabling the fabrication of living constructs with spatially controlled architectures. By depositing bioinks in a layer-by-layer fashion according to a digital blueprint, it is possible to reproduce aspects of tissue organization and function (Zeng *et al.*, 2022; Bao *et al.*, 2020). A central goal in the field is the creation of constructs that not only match the geometry of target tissues but also replicate their porous structure and viscoelastic properties, which strongly influence cell adhesion, proliferation, differentiation, and migration (Wu *et al.*, 2022; Wei *et al.*, 2020; Chen *et al.*, 2017; Parmar *et al.*, 2016; Courbot & Elosegui-Artola, 2025). Despite rapid progress, the fabrication of highly complex and functional constructs remains limited by the printability of soft, low-viscosity, or slow-crosslinking bioinks. These materials, while often biologically relevant, collapse upon extrusion, yielding poor shape fidelity and resolution (Schwab *et al.*, 2020).

To overcome these challenges, embedded bioprinting was developed, in which bioinks are extruded into a secondary material, or support bath, that temporarily holds the printed material in place until it crosslinks (Hinton *et al.*, 2015; Highley *et al.*, 2015; Bhattacharjee *et al.*, 2015). This approach enables the use of a broader range of bioinks, including those that more closely mimic the native extracellular matrix, and facilitates the creation of freeform and overhanging features. Several support bath materials have been reported, such as gelatin microparticles in the Freeform Reversible Embedding of Suspended Hydrogels (FRESH) technique (Hinton *et al.*, 2015), gellan gum fluid gels (Compaan *et al.*, 2019), carbopol hydrogels (Hinton *et al.*, 2016), agarose slurries (Cidonio *et al.*, 2019), and pluronic blends (Rahimnejad *et al.*, 2022; Hu *et al.*, 2023). While each system has enabled important advances, common limitations

remain, including insufficient oxygen and nutrient transport restricting long-term viability, and challenges with bath removal without damaging the construct (Lee *et al.*, 2019; Shiwarski *et al.*, 2021).

Recently, in-foam bioprinting has been introduced as a promising alternative, in which mechanically foamed albumin in cell culture media is used as the support bath (Madadian *et al.*, 2024b). Albumin foams offer unique biological advantages: the gas bubbles facilitate oxygen delivery, the aqueous phase maintains nutrient availability, and the inherent instability of foams allows for self-removal of the support without additional processing. Madadian et al. demonstrated that albumin foams possess rheological properties compatible with embedded bioprinting and could sustain high cell viability. However, their practical application is limited by rapid degradation, which restricts the time window for printing more complex or large-scale constructs.

Foam stabilization has been studied extensively in the food and colloid sciences, where it is well established that protein-based foams can be reinforced by the addition of polysaccharides (Schmidt *et al.*, 2010; Sadahira *et al.*, 2015). Pectin, a high–molecular weight, anionic polysaccharide, is particularly attractive due to its biocompatibility and its ability to increase viscosity, form polymer entanglements in the continuous phase, and interact with proteins at the air–liquid interface (Miquelim *et al.*, 2010; Zhang *et al.*, 2023b). Beyond its role as a stabilizer in food foams, pectin has been widely investigated for biomedical applications such as wound healing (Amante *et al.*, 2023), drug delivery (Méndez *et al.*, 2023), and tissue engineering (Eivazzadeh-Keihan *et al.*, 2022; Morello *et al.*, 2023). These properties suggest that pectin could improve foam stability without compromising the biological compatibility required for bioprinting applications.

In this study, we investigated the incorporation of pectin into albumin foams to extend their stability as embedded bioprinting support baths. We hypothesized that pectin would reduce drainage and bubble coalescence while preserving the rheological properties essential for printing. Albumin-only foams (A8) were compared with albumin foams containing 1% or

2% pectin (A8P1, A8P2). Foam stability, bubble morphology, rheology, and physicochemical properties were characterized, and the printability of chitosan—a representative low-viscosity, slow-crosslinking hydrogel—was assessed. Finally, cell viability in printed fibroblast constructs was evaluated in comparison to traditional FRESH baths. Together, these experiments provide evidence that pectin-stabilized albumin foams represent a versatile and biologically favorable support system for embedded bioprinting.

2.3 Materials and Methods

2.3.1 Foam Preparation

The foam was prepared by dissolving albumin powder from chicken egg white (A5253, Sigma-Aldrich, USA) and pectin powder from citrus peel (galacturonic acid ≥ 74.0%, P9135, Sigma-Aldrich, USA) in either deionized (DI) water or Dulbecco's Modified Eagle Medium (DMEM) (Gibco^{TM} DMEM/F-12, Thermo Fisher Scientific) supplemented with 10% v/v Fetal Bovine Serum (FBS) and 1% v/v antibiotics penicillin/streptomycin henceforth referred to as complete DMEM. Pectin powder was added to the solvent first and stirred at 600 rpm until completely dissolved. Albumin powder was then added, and the solution was stirred at 600 rpm for an additional 3 hours to ensure complete dissolution. The solution was then mechanically mixed at 2000 rpm for 2 minutes using a Cole-Parmer OS-200D-C-SYS Compact Digital Mixer System (Cole-Parmer Instrument Company, Vernon Hills, IL, USA) immediately prior to all tests. Three compositions of foam were prepared for each test: 8% w/v albumin (A8), 8% w/v albumin with 1% w/v pectin (A8P1) and 8% w/v albumin with 2% w/v pectin (A8P2).

Table 2.1 Compositions of the foam support baths studied

	Albumin (% *w/v*)	**Pectin (% *w/v*)**
A8	8	0
A8P1	8	1
A8P2	8	2

2.3.2 Foam Stability

To quantify the liquid drainage of the foam over time, the foam was loaded into 15 mL Falcon tubes using a syringe immediately following its preparation. The Falcon tubes were then secured inside a water bath set to 37°C for the duration of the test. The volume of the liquid drainage accumulated at the bottom of the Falcon tube was measured at distinct time points: 0, 5, 10, 15, 20, 25, 30, 40, 50, 60, 90 and 120 minutes from the time the foam was prepared. For better visualization of the liquid drainage over time, as well as to see the change in bubble size over time, foams were additionally transferred into ultraviolet (UV) quartz cuvettes (Sigma-Aldrich, Oakville, ON, Canada) using a syringe immediately after their preparation and photographed at various time points.

2.3.3 Foam Bubble Size

A brightfield microscope (RVL-100-G, Echo, San Diego, CA, USA) set to 4x magnification was used to image the bubble size of the foams at various time points starting immediately after mechanically foaming: 0, 10, 30, 60, and 120 minutes. The foam was kept in a sealed container over the course of the experiment and a new small sample was retrieved and gently spread as a thin layer on a petri dish for imaging at each time point. This technique was used as opposed to imaging the same sample over time to ensure that the foam being imaged did not dry out, which would not properly represent the natural breakdown of foam as experienced in the in-foam bioprinting setup. For each foam composition and each time point a minimum of 3 images were taken at different locations of the sample and the diameter of a minimum of 600 bubbles were measured using ImageJ software.

2.3.4 Foam Overrun

Foam overrun percentage was used to quantify the foamability of each foam composition (i.e. the increase in volume of the foam compared to its original liquid volume). After dissolving the powdered pectin and albumin, 15 mL of the liquid was weighed. The solution was then

mechanically foamed at 2000 rpm for 2 minutes and 15 mL of the resulting foam was weighed. The overrun % was calculated using equation (2.1) as

$$\text{overrun } (\%) = \left(\frac{m_i - m_f}{m_f} \right) \times 100 \tag{2.1}$$

where ml is the mass of the liquid prior to mechanical foaming and mf is the mass of the resulting foam after mechanically foaming (Sadahira *et al.*, 2015).

2.3.5 Rheology

All rheological testing was performed on an Anton Paar rheometer (Physica MCR 301, Germany) with concentric cylinder geometry (CC10/T200). All tests were performed at 37°C. The rheological properties of the foams were characterized using the tests outlined in the following subsections.

2.3.5.1 Viscosity

The viscosity of the foams (A8, A8P1, and A8P2) was measured over varying shear rates from 0.01-100 s^{-1} to confirm the foam supports exhibited shear thinning behavior. The results are plotted using a logarithmic scale.

2.3.5.2 Recovery

The self-recovery properties of the foam supports were characterized through cyclic recovery tests. The test was designed to mimic the cycles of deformation experienced by the foam support as the print needle passes through and returns layer-by-layer. The storage modulus (G') of each foam (A8, A8P1, and A8P2) was measured through several cycles of the following: 30 seconds at 1% strain followed by 30 seconds at 100% strain followed by a sudden return to 1% strain for 30 seconds (Rahimnejad *et al.*, 2022; Madadian *et al.*, 2024b). The intervals at 1% strain mimic before and after the printing process whereas the intervals of 100% strain mimic the print needle passing through and deforming the foam.

2.3.6 Physiochemical Characterization

2.3.6.1 pH

The pH of the following components of each foam composition were measured using a pH meter (LAQUAtwin, Horiba Advanced Techno, Kyoto, Japan): the liquid solution prior to mechanical foaming, the foam created from the mechanical mixing and the liquid drainage from foam as it breaks down collected from the bottom of the vessel containing the foam.

2.3.6.2 Osmolality

The osmolality of each foam composition was measured using an automated single-sample osmometer (3320, Advanced Instruments, Inc.). The osmometer was calibrated using a Clinitrol^{TM} 290 reference solution (Advanced Instruments Inc., Massachusetts, USA) which has an osmolality close to physiological levels. The osmolality was measured and is reported in milliosmoles per kilogram (mOsm/kg). The liquid solution containing dissolved albumin on its own and with either 1% w/v or 2% w/v pectin before mechanical foaming were measured. Additionally, the liquid drainage resulting from the degradation of each foam composition were measured.

2.3.7 Chitosan Hydrogel Preparation

A physical thermosensitive chitosan hydrogel with gelling agent was used for both printability studies and cell studies. The chitosan was prepared following a previously published protocol (Assaad, Maire & Lerouge, 2015; Ceccaldi *et al.*, 2017; Touani *et al.*, 2025). Briefly, shrimp shell chitosan powder (ChitoClear, HQG110, Primex, Siglufjordur, Iceland) with a molecular weight of 159 kDa and degree of deacetylation of 74% was dissolved in 0.1 M hydrochloric acid (HCl) (Fisher Scientific) using an overhead stirrer for 4 hours then autoclaved at 121oC for 20 minutes for aseptic conditions. The gelling agent was prepared by dissolving -glycerol phosphate (GP, Sigma-Aldrich, USA) and sodium hydrogen carbonate (SHC, Merck KGaA, Germany)

in DI water, and subsequently sterilized by filtration using a 0.22 µm pore size syringe filter (UltiDent Scientific, Canada). Both the pH of the chitosan and the gelling agent were measured using a pH meter (LAQUAtwin, Horiba Advanced Techno, Kyoto, Japan) to ensure they were in the proper ranges for use (the chitosan was only used if the pH was between 6-6.3 and between 7.4-8.4 for the gelling agent). Mixing both solutions leads to a gel precursor solution with physiological pH to which the cell suspension can be added. In the printability tests, the cell suspension was substituted with Phosphate-Buffered Saline (PBS) 1X. Each component of the hydrogel was mixed using syringes connected by a luer lock immediately prior to printing. The volume ratio of 3:1:1 of chitosan to gelling agent to cell suspension. This led to a hydrogel final composition of 2% w/v Chitosan, 0.1 M GP and 0.75 M SHC. This specific composition was selected because it leads to an in situ gelling hydrogel with strong mechanical properties, interconnected porosity and good cell survival and growth (Assaad *et al.*, 2015; Ceccaldi *et al.*, 2017; Touani *et al.*, 2025). However, it is slow crosslinking and has a low viscosity at room temperature prior to gelation. This means the chitosan must be physically supported once extruded through the print needle to maintain its shape for gelation.

2.3.8 Printability

A BioX pneumatic extrusion bioprinter (Cellink, Gothenburg, Sweden) was used with a either a ½" or 1" long 22 G stainless steel blunt printing needle (McMaster-Carr, Elmhurst, IL, USA) with 5 mm/s printing speed and 15 kPa pressure for all printability tests. The printing pressure of 15 kPa was selected based on preliminary optimization tests, which showed that this pressure provided the most consistent and continuous extrusion of the low-viscosity chitosan bioink while avoiding over-extrusion at higher pressures and discontinuous filament formation at lower pressures. A 2% w/v chitosan hydrogel without cells, as described in section 2.3.7, was used for the printability study. The printhead containing the hydrogel filled cartridge was at room temperature and the print bed filled with foam was set to 37°C permitting the chitosan to begin gelling immediately after being printed. Once the printed constructs were fully gelled, the foam support bath was removed using a Pasteur pipette and negative pressure. Various structures

were printed to test the printability within the foam supports including, grids patterns, free-form conical structures and structures with overhanging features.

2.3.9 Cell Studies

2.3.9.1 Cell Culture

Mouse fibroblast L929 cells (ATCC 1 CCL-1 from Mouse Batch number 70026472) were cultured in a humidified incubator at 37°C and 5% CO_2 using complete DMEM. Cells, passage 8 to 13, were subcultured into a new T75 flask upon reaching 80% confluency and detached using 0.05% trypsin/EDTA. The cell media were replaced with fresh media every 2-3 days to ensure the cells had continuous access to nutrients.

2.3.9.2 Chitosan Bioink Preparation

The 2% w/v chitosan bioinks outlined in section 2.3.7 consisted of a 3.33% w/v chitosan solution combined with a gelling agent solution containing 0.5 M βGP and 0.375 M SHC which was then encapsulated with L929 cells. Using two syringes connected by a luer lock, the chitosan and gelling agent were mixed together with 15 back-and-forths. The resulting mixture was then mixed with the cell suspension using the same technique. A 3:1:1 (chitosan: gelling agent: cell suspension) ratio was used, resulting in a bioink with the following final concentration: 2% w/v chitosan, 0.1 M βGP, 0.075 M SHC and either 2 or 3 M cells/mL.

2.3.9.3 Cell Viability

The first cell study completed was to investigate if the addition of pectin had any impact on the viability of the cells encapsulated in the printed bioink. The cell laden bioink with, 3 M cells/mL, was used to extrusion print a filament the three foam compositions (A8, A8P1 and A8P2) and left for 30 minutes outside of the incubator, at room temperature after which the foam was removed, rinsed with PBS 1X then complete DMEM was added to the cell-laden constructs

which were then placed in the humidified incubator at 37°C and 5% CO_2. As a positive control, Control A, the bioink was printed outside of the foam, supplemented immediately with complete DMEM, and transferred directly to the incubator to demonstrate cell viability under standard culture conditions. A negative control, Control B, consisted of printing the bioink outside of the foam then waiting either 30 minutes or 1 hour before adding cell culture media and being placed in the incubator. This control mimicked what encapsulated cells would experience during a long print taking place in open air and outside of a nutrient enriched foam bath.

A second cell study was performed to compare the cell viability when the cell-laden bioinks were printed and left in the different support baths over long periods of time. The foam supports were compared to a traditional support bath material: a gelatin microparticle slurry as used in the FRESH technique. Two versions of a FRESH support were used: one prepared using complete media as the aqueous phase (DMEM FRESH), and the other using PBS 1X (PBS FRESH). Both formulations were prepared using a previously published protocol (Hinton *et al.*, 2015) using Type A gelatin from porcine skin (MilliporeSigma, USA). Briefly, 4.5% w/v gelatin was dissolved in either complete DMEM or PBS 1X then gelled at 4°C for 12 hours. Subsequently, media or PBS was added to the gel and was blended for 2 minutes at pulse speed using a consumer-grade blender (Hamilton-Beach). The blended solution was then centrifuged, after which the supernatant was removed and replaced with fresh media or PBS then vortexed back into suspension. These steps were repeated until there were no more bubbles at the top of the solution after centrifugation. The chitosan bioink loaded with 2 M cells/mL, was extrusion bioprinted to create a filament into each of the 5 supports being tested: A8, A8P1, A8P2, DMEM FRESH and PBS FRESH. The printed constructs were left in the support for either 3 or 5 hours at room temperature after which the supports were removed, rinsed with PBS 1X then complete DMEM was added. The prints were then placed in the humidified incubator at 37°C and 5% CO_2.

A live/dead cell viability assay was used 24 hours after the printing process to examine the viability of L929 cells embedded in the printed chitosan hydrogel for both cell studies. 2 μM of Calcein, AM (Invitrogen, Life Technologies, Carlsbad, CA, USA) and 5.5 μM of Ethidium

Homodimer-1 (EthD-1, Invitrogen, Life Technologies, Carlsbad, CA, USA) in serum free DMEM were used to stain the live and dead cells respectively. The cell-laden models were incubated with the stains for 45 minutes before removing the stain, rinsing with PBS 1X, and then submerging in serum-free DMEM for imaging using a fluorescence microscope (RVL-100-G, Echo, San Diego, CA, USA). Three images were taken at random locations of each sample. ImageJ was used to analyze all fluorescent cell images. The green (live cells) and red (dead cells) channels of each image were normalized using a greyscale filter and appropriate thresholding of contrast and brightness levels allowed for measurements of the projected area of the red and green signals. The cell viability percentage was calculated using equation (2.2):

$$\text{Cell Viability } \% = \left(\frac{\text{live cells}}{\text{live cells + dead cells}} \right) \times 100 \tag{2.2}$$

2.3.10 Dissolved Oxygen Levels

The levels of dissolved oxygen in the support baths were measured using a non-invasive optical oxygen meter (Fibox 4, PreSens Prescision Sensing GmbH, Germany) equipped with PSt3 planar oxygen sensor spots (SP-PSt3-NAU, PreSens Precision Sensing GmbH, Germany) and a polymer optical fiber (PreSens Precision Sensing GmbH, Germany). The sensor spots were glued to glass cover slips with a silicone glue (SG2 silicone glue, transparent, Presens Precision Sensing GmbH, Germany) and positioned on the surface where cell-laden constructs were printed in one of the following supports: A8, A8P1, or FRESH support bath prepared with DMEM. The salinity of each support bath was measured using an Oakton^{TM} PC 2700 Benchtop Meter (Oakton Instruments, USA). Dissolved oxygen measurements were taken at various time points starting immediately after the printing as well as at after 1 hour, 3 hours, 5 hours and 8 hours.

2.3.11 Chitosan Microstructure Analysis

2.3.11.1 Scanning Electron Microscopy (SEM)

Using the same chitosan hydrogel as in the printability studies (see section 2.3.8), multi-layered grids were 3D bioprinted either in an A8P1 foam support or directly onto a printing surface without a foam support. The printed structures were left in the foam for 5 hours before removing the foam, adding complete DMEM, then placing them in the incubator at 37°C. The constructs printed outside of the foam were immediately incubated at 37°C for 10 minutes to initiate gelation, after which complete DMEM was added. 24 hours after printing, the hydrogels were freeze-dried (Harvest Right) overnight. The freeze-dried samples were then secured on SEM imaging stubs using conductive tape and sputter-coated with a 20 nm gold layer (K550X Sputter Coater) and imaged using SEM S3600-N Hitachi (15 kV).

2.3.11.2 Histology

Similar grids were also prepared for histology. After incubation at 37°C for 24 hours to allow for complete gelation, the samples were gently washed with PBS 1X, fixed in 10% formalin for 5 minutes, and embedded in HistoGel™ (Thermo Fisher Scientific, USA). Samples were then enrobed in paraffin, sliced at 4 μm thickness and stained with hematoxylin and eosin (H&E) following standard histological protocols. The microstructures were examined on high resolution scan images using the Aperio ImageScope software (Leica Biosystems, IL, USA).

2.3.12 Statistical Analysis

All reported results represent mean values +/- standard deviations of tests done at least in triplicate. The Shapiro-Wilk test was used to test for normality and skewness of the data, and Levene's test was used for equal variance. Statistical analysis of all data, except for bubble size, was performed using analysis of variance (ANOVA), with Tukey's HSD post hoc analysis to compare every two groups of data. For bubble size, Kruskall-Wallis was used, and Dunn's post

hoc analysis was used to compare every two groups of data. For each test, p-values below 0.05 were considered statistically significant. All statistical analysis calculations were performed in RStudio.

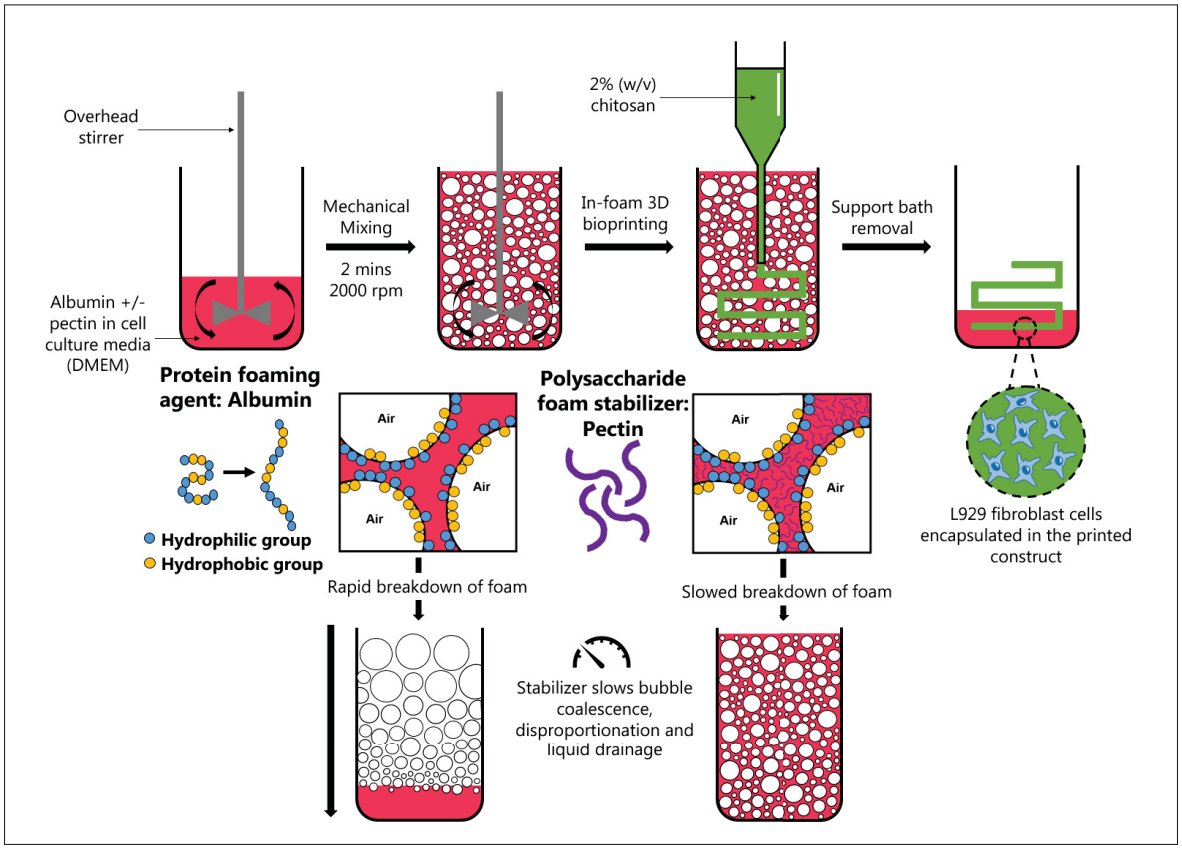

Figure 2.1 Schematic illustrating the in-foam bioprinting process with pectin acting as a stabilizer for the albumin-based foam

2.4 Results and Discussion

Each composition of foam studied (A8, A8P1, A8P2) contained 8% albumin and a mechanical foaming time of 2 minutes was chosen for all foams since previous studies have shown it provides the best results for embedded bioprinting applications (Madadian *et al.*, 2024b). Further, when higher concentrations of albumin were tested with pectin the solution became too thick, and foaming became difficult. With lower than 8% albumin, the foam was visibly less stable with liquid draining from the foam immediately after preparation.

2.4.1 Foam Stability, Bubble Size and Foamability

The effects of pectin addition on the physical stability of albumin foams are summarized in Figure 2.2. As shown in Figure 2.2(a)–(b), A8 (albumin-only) foams underwent rapid liquid drainage, with visible phase separation occurring within the first minute after foaming. In contrast, the onset of drainage was delayed to 30 minutes for A8P1 and to nearly 60 minutes for A8P2. This can also be seen with the quantitative measurements in Figure 2.2(b), demonstrating that higher pectin concentrations significantly reduce drainage rates, extending foam lifetime.

Bubble size evolution further reflects this stabilizing effect (Figure 2.2(c)–(e)). A8 exhibited a wide bubble size distribution immediately after foaming and rapid coalescence over 120 minutes, producing larger, heterogeneous bubbles. By comparison, both A8P1 and A8P2 maintained smaller and more uniform bubbles over time, with the 2% pectin formulation showing the narrowest distribution and slowest growth.

Foamability, measured by overrun percentage, decreased with increasing pectin concentration (Figure 2.2(f)). While A8 produced the highest expansion, A8P1 and A8P2 generated progressively lower overrun values. This reduction is attributed to increased viscosity of the liquid phase with pectin addition, which restricts gas incorporation during whipping but enhances stability once bubbles are formed.

Taken together, these results demonstrate that pectin enhances albumin foam stability by slowing drainage and coalescence while narrowing bubble size distribution. The stabilization arises from physical mechanisms at multiple scales: (i) increased viscosity of the aqueous phase slows liquid drainage, (ii) protein–pectin complexes accumulate in the foam lamellae and Plateau borders, strengthening interfacial films against rupture, and (iii) electrostatic and steric repulsion from the polysaccharide chains hinder bubble coalescence. Similar synergistic effects of protein–polysaccharide complexes have been reported in food foams (Schmidt *et al.*, 2010) and in model systems where pectin reduces drainage and disproportionation through viscosity and interfacial reinforcement (Sadahira *et al.*, 2015).

It is important to note, however, that although the A8P2 composition was able to foam and created a stable foam, increasing the concentration of pectin beyond 2% w/v is not ideal. At elevated concentrations, the liquid phase becomes excessively viscous, making it increasingly difficult to incorporate air and disperse gas into bubbles during whipping. This results in poor foamability, as reflected in the lower overrun values observed with 2% pectin. Therefore, while pectin enhances stability, there is an optimal concentration window beyond which the trade-off between foamability and stability becomes unfavorable.

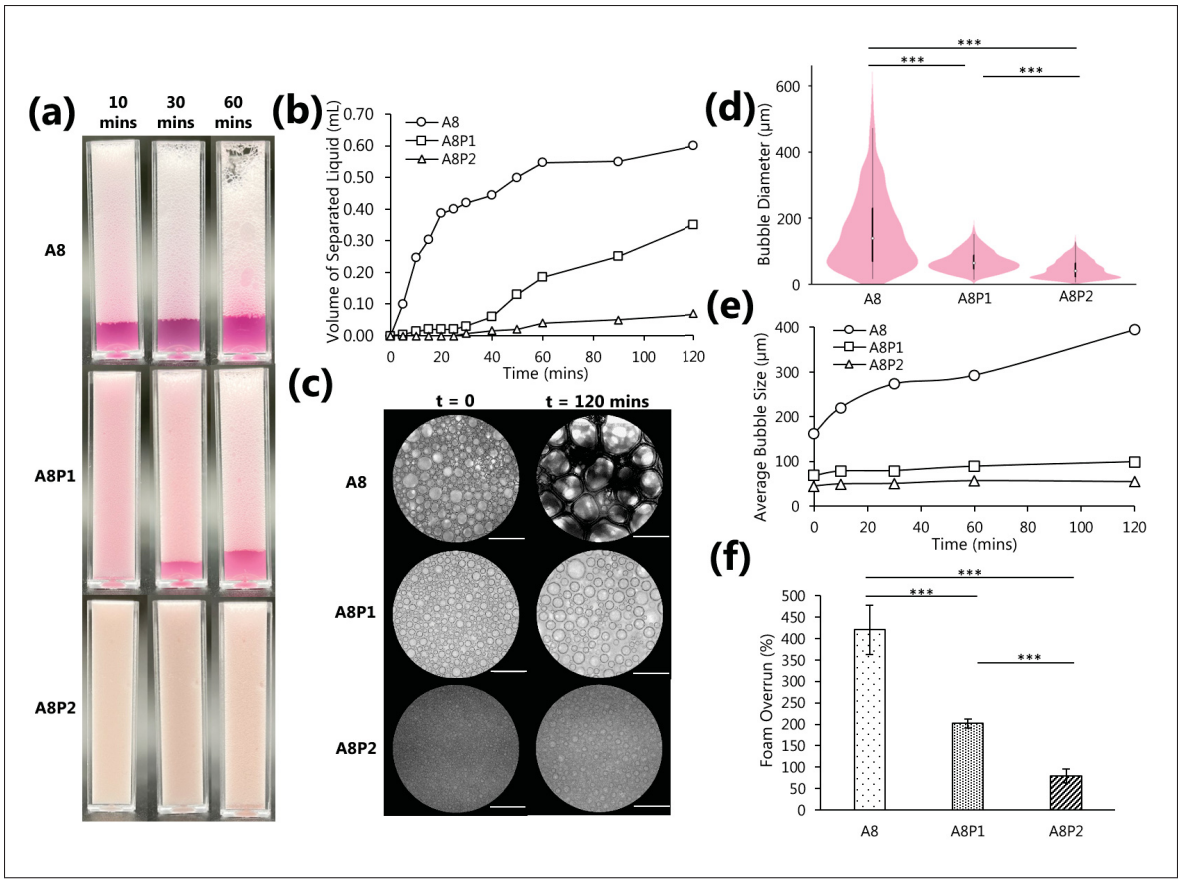

Figure 2.2 Physical characterization of the foam support baths. (a) Liquid drainage of foams over time (b) Quantification of liquid drainage overtime from the foam in the Falcon tubes (mean values of triplicates are plotted) (c) Difference in initial bubble size and bubble size after 2 hours (Scale bars: 1 mm) (d) Initial bubble size distribution (e) Average bubble size over time (f) Overrun % of the foams (mean +/- SD, $n = 5$, $*p < 0.05$, $**p < 0.01$, $***p < 0.001$)

2.4.2 Rheology

For a material to be acceptable as a support bath in embedded bioprinting, it must possess key rheological properties, particularly shear-thinning behavior and the ability to recover its mechanical strength after repeated deformations. Figure 2.3 illustrates these properties for the albumin–pectin foams. Viscosity measurements (Figure 2.3(a)) confirmed that all foam formulations were shear-thinning, a critical property for embedded bioprinting because it permits free nozzle movement during extrusion while ensuring the bath quickly recovers its solid-like, supporting structure once the nozzle is gone (Budharaju *et al.*, 2024). The increase in low-shear viscosity with pectin addition improves the stability of the bath without compromising flowability under shear. These rheological features are consistent with previous reports on protein–polysaccharide complexes, which increase the viscoelasticity of the continuous phase and reinforce lamellae to improve foam recovery after deformation (Schmidt *et al.*, 2010; Sadahira *et al.*, 2015). The higher viscosity measured for the A8 foam can be attributed to the rapid degradation of the foam causing it to dry slightly during the measurement, increasing the measured viscosity.

In the cyclic recovery tests (Figure 2.3(b)), all foams were able to recover their storage modulus (G') after successive cycles of strain, which simulates the passage of the print nozzle during deposition. Notably, A8P1 and A8P2 exhibited higher overall recovery of G' compared to the albumin-only foam (A8), indicating that pectin improves the resilience of the foams to repetitive deformation. This higher recovery is likely due to pectin reinforcing the bubble interfaces, allowing bubbles to stretch elastically without rupturing. In contrast, the faster liquid drainage in A8 causes it to lose structural integrity more quickly, leading to poorer recovery, consistent with earlier findings on albumin foams (Madadian *et al.*, 2024b). Compared to conventional gelatin microparticle baths used in FRESH bioprinting, the albumin–pectin foams provide a comparable rheological response but with the added advantages of oxygen diffusion and higher long-term cell viability. Thus, pectin-containing albumin foams retain the desirable rheological behavior of albumin-only foams while extending their stability and functionality for embedded bioprinting.

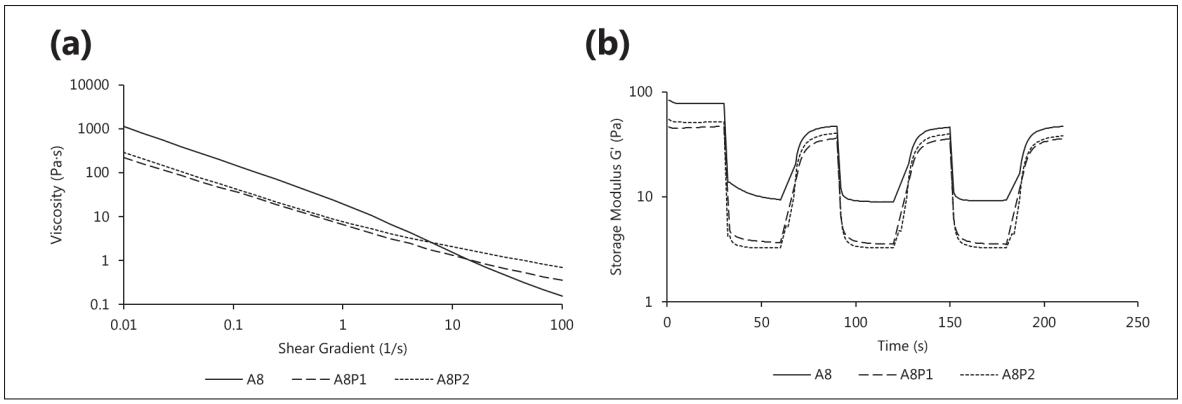

Figure 2.3 Rheological characterization of the foam supports. (a) Shear thinning tests: the viscosity of the foam supports as a function of shear gradient (b) Recovery tests: storage moduli of the foam as a function of time through several cycles of applied strain (30 s 1% strain followed by 30 s at 100% strain repeated) (mean values of triplicates are plotted)

2.4.3 Printability

Chitosan, a low-viscosity and slow-crosslinking hydrogel, was printed in the albumin–pectin foams to evaluate their ability to support challenging bioinks (Figure 2.4). The pectin-stabilized foams successfully supported multilayered and freeform structures, including filaments with overhanging features. By contrast, the same chitosan hydrogel printed outside of a support bath exhibited poor print fidelity, with even simple filaments collapsing immediately. This highlights the critical role of the support bath in enabling the use of hydrogels like chitosan, which, despite their poor standalone printability, are attractive for tissue engineering due to their biocompatibility, biodegradability (Kumar *et al.*, 2023), antimicrobial activity (Deng, Wang, Chen & Liu, 2020; Jiménez-Gómez & Cecilia, 2020), and tunability (Babu, Shanmugavadivu & Selvamurugan, 2024).

Chitosan is a polycationic polymer that is positively charged in acidic to near-neutral conditions (Yadav, Kaushik, Rao, Srivastava & Vaya, 2023). Given that albumin carries a net negative charge in the pH range of the foams (pH levels well above 4.7 which is the isoelectric point of albumin (Guha, Majumder & Mine, 2019)) used here, a thin residue was observed on the surface of constructs after bath removal. Because this residue interferes with quantitative shape analyses,

print fidelity was assessed qualitatively rather than using a printability number (Pr = $L^2/16A$ (Madadian, Naseri, Legault & Ahmadi, 2024a)) visual inspection indicated that the constructs printed in pectin-containing foams were of comparable quality to those reported in albumin-only foam supports (Madadian *et al.*, 2024b) and were consistent with other embedded bioprinting methods using granular or gel-based baths (Rahimnejad *et al.*, 2022).

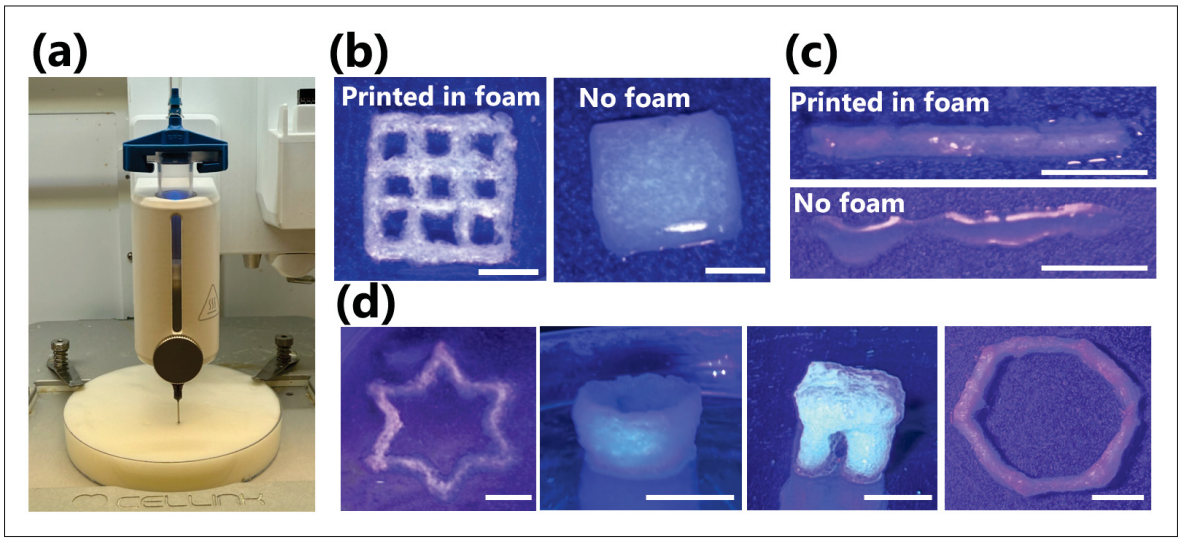

Figure 2.4 (a) In-foam bioprinting setup using a Cellink BIO X 3D bioprinter and 22 G print needle (b) (left) chitosan grid printed in A8P1foam (right) same grid printed outside of foam support demonstrating poor printability (c) (top) filament printed in foam (bottom) filament printed outside of foam with poor printability (d) various geometries printed using chitosan into the foam supports. All scale bars are 1 cm

2.4.4 Cell Viability

The first cell viability study examined whether the addition of pectin in the foam influenced the viability of chitosan-encapsulated L929 fibroblasts. As shown in Figure 2.5, constructs printed in pectin-containing foams (A8P1 and A8P2) exhibited high cell viability, with A8P1 (1% pectin) achieving the highest viability among the three foam supports tested. The addition of pectin therefore did not negatively impact cell health. This result was expected, as pectin is well documented to be biocompatible and has been widely investigated in biomedical applications such as drug delivery, wound healing, and tissue engineering (Zhang *et al.*, 2023b; Sultana, 2023).

These findings are also consistent with Madadian *et al.* (2024b), who reported that cell-laden constructs printed in albumin foam maintained high viability over time before replacement with media.

The experimental design included two controls for comparison (Section 2.3.9.3). Control A represented standard culture conditions, where constructs were printed outside of the foam, immediately supplemented with media, and placed in the incubator. Control B mimicked an extended print in open air: constructs were printed outside of the foam, left without media for both 30 minutes and one hour, and only then supplemented and incubated. In contrast, in-foam printed constructs were left in the albumin or albumin–pectin foams for 30 minutes before the support was removed, media was added, and the samples were transferred to the incubator. As illustrated in Figure 2.5, both Control Bs (left for 30 minutes and 1 hour) showed a drastic reduction in cell viability due to nutrient deprivation and desiccation, whereas constructs printed in the foams retained high viability. This highlights a critical advantage of in-foam embedded bioprinting: the support not only stabilizes the bioink mechanically but also provides a temporary nutrient-rich microenvironment that protects cells during and immediately after the printing process.

In the second viability study (methods described in Section 2.3.9.3), cell-laden constructs were bioprinted directly into the different support baths and left in place for either 3 or 5 hours before the supports were removed and fresh media was added. The supports tested included the three foam formulations (A8, A8P1, A8P2) and two gelatin microparticle slurries prepared according to the FRESH protocol (one with DMEM and one with PBS as the aqueous phase). This setup was designed to mimic long print durations in which cells remain embedded in the support bath for extended periods prior to media exchange.

The results are presented in Figure 2.6. After 3 hours, constructs printed in all three foams maintained high cell viability, while those printed in either version of the FRESH support exhibited poor viability. At 5 hours, A8 and A8P1 still supported acceptable viability, whereas A8P2 and both FRESH conditions showed a pronounced decline. This limited long-term

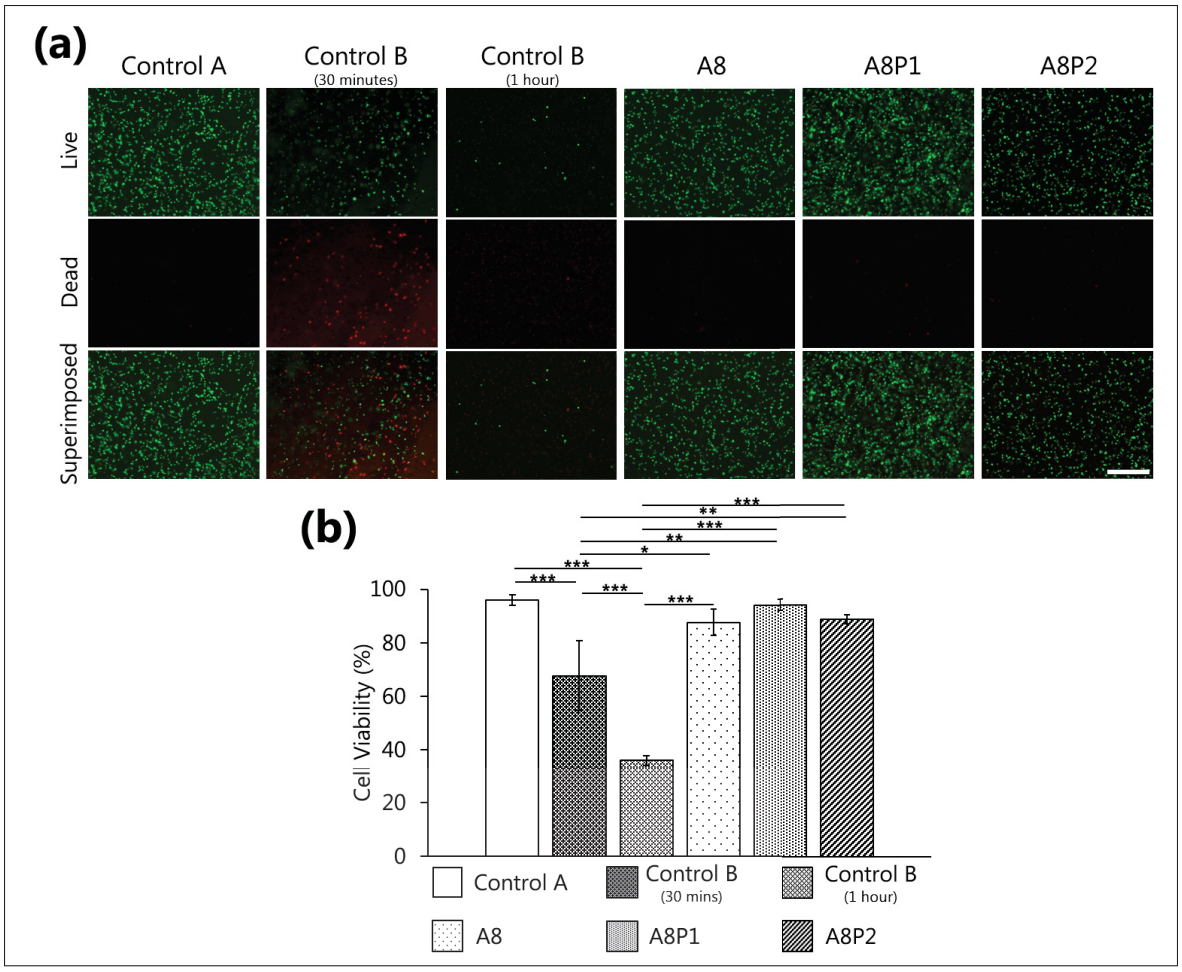

Figure 2.5 Impact of the addition to pectin to albumin-based foam on cell viability in chitosan bioinks. (a) Live/dead fluorescence microscopy images and (b) quantified cell viability results 24 hours after the printing process. Scale bar is 200 m. (mean +/- SD, $n = 3$, *$p < 0.05$, **$p < 0.01$, ***$p < 0.001$)

performance of gelatin microparticle baths has also been reported elsewhere; for example, Bessler *et al.* (2019) observed a drop in HEK293 cell viability from 81% after one hour to 48% after two hours in a FRESH slurry (Bessler *et al.*, 2019).

These short-term cell viability studies were designed specifically to assess whether the support bath environment itself had any immediate cytotoxic or mechanical effects on the printed constructs. Long-term cell culture studies were therefore beyond the intended scope of this work, as the influence of the support bath becomes negligible once the construct is fully removed and

is cultured under standard conditions for several days. Moreover, the long-term biocompatibility of the 2% chitosan bioink formulation used in this work has already been validated with several cell types in the past (Ceccaldi *et al.*, 2017; Touani *et al.*, 2025; Alinejad *et al.*, 2019).

To further explain these findings, dissolved oxygen levels were measured in selected baths during incubation of printed constructs. A8P2 and PBS-based FRESH were excluded due to their poor viability results, leaving A8, A8P1, and DMEM-based FRESH for comparison. Foam-based supports maintained higher oxygen levels with only small decreases over time, while the FRESH bath exhibited a substantial drop (Figure 2.6(c)). This supports the hypothesis that the porous bubble network in foams facilitates oxygen delivery, whereas the dense gelatin microparticle matrix impedes diffusion and may also hinder waste removal, leading to hypoxic conditions and reduced cell survival during extended print times. It is important to note that in this experiment, the thickness of the foam covering the printed construct was relatively thin as the experiment took place in a 24 well plate. It is hypothesized that the drop in dissolved oxygen levels would be even worse given thicker coverage of the printed construct by the support bath.

2.4.5 Physiochemical Characterization

The physiochemical properties of the foams are presented in Figure 2.7. Increasing pectin concentration led to a progressive decrease in pH, consistent with the acidic nature of galacturonic acid residues in pectin (Mudgil, 2017). The A8 foam had a pH of 8.44 ± 0.13, which is higher than the physiological range of 7.35–7.45 (Hopkins, Sanvictores & Sharma, 2018). This alkalinity arises from using DMEM to prepare the foam which uses a sodium bicarbonate buffering system that requires a high levels of to maintain physiological pH. Since the foam is prepared outside an incubator, the absence of elevated CO levels (5–10% normally used in culture conditions) permits CO escape, thereby increasing the pH. The stirring and high-speed mixing steps further accelerate this degassing.

In contrast, the A8P1 formulation (pH 7.71 ± 0.18) was much closer to physiological conditions and corresponded to the highest cell viability observed in Section 3.4.4. A8P2 was slightly

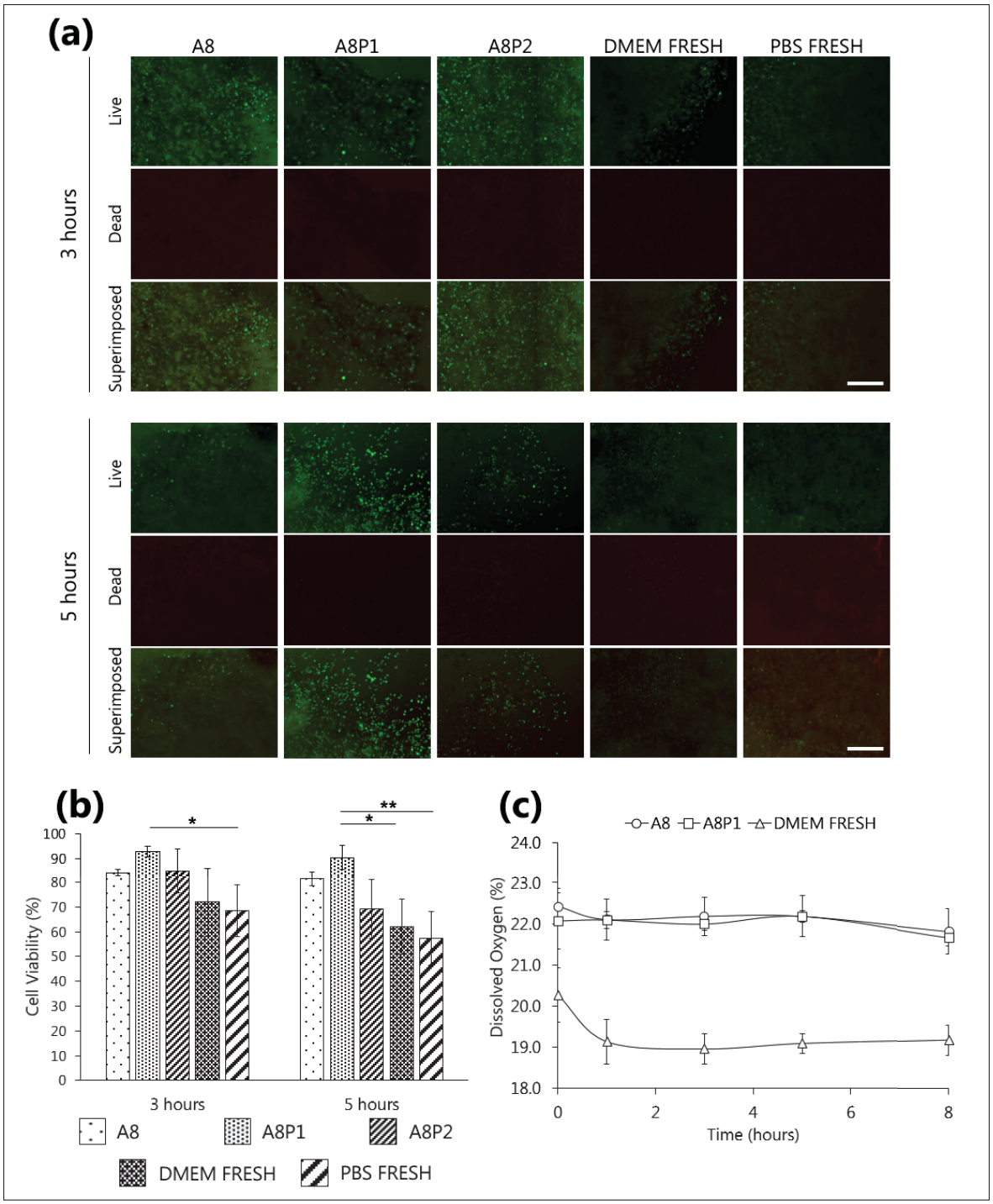

Figure 2.6 Comparison of foam support baths to FRESH bioprinting. L929 cells embedded into a chitosan hydrogel were printed and left in A8, A8P1, Alp8P2, and a FRESH support bath prepared with either DMEM or PBS 1X and left for 3 hours and 5 hours before replacing the support bath with cell media. (a) Fluorescent microscopy images and (b) quantification of live/dead assays completed after 24 hours. (c) Dissolved oxygen content in the support baths over time with the mean value of triplicates plotted +/- SD. Scale bars are 200 μm. (mean +/- SD, $n = 3$, $*p < 0.05$, $**p < 0.01$, $***p < 0.001$)

acidic (pH 6.72 ± 0.05), which correlated with reduced viability. This trend reflects the known sensitivity of L929 fibroblasts, which tolerate mildly alkaline conditions better than acidic ones. Indeed, Gunnink *et al.* (2014) reported that increasing extracellular pH from 6 to 9 enhanced glucose uptake in these cells six-fold, suggesting greater metabolic activity under slightly basic conditions (Gunnink *et al.*, 2014). Together, these findings explain why A8P1 produced the most favorable microenvironment, followed by A8, while A8P2 was less supportive.

To confirm that pH was the main differentiating factor, the pH of the precursor solutions, foams, and drainage liquids was measured, with no statistically significant differences found between these components within each formulation. Osmolality measurements further showed no significant increase with the addition of pectin, indicating that the observed differences in cell viability are more likely attributed to pH shifts rather than osmotic stress. Overall, these results reinforce the close link between foam composition, physicochemical environment, and biological outcomes, highlighting the importance of tuning pH through stabilizer concentration for optimizing in-foam bioprinting applications.

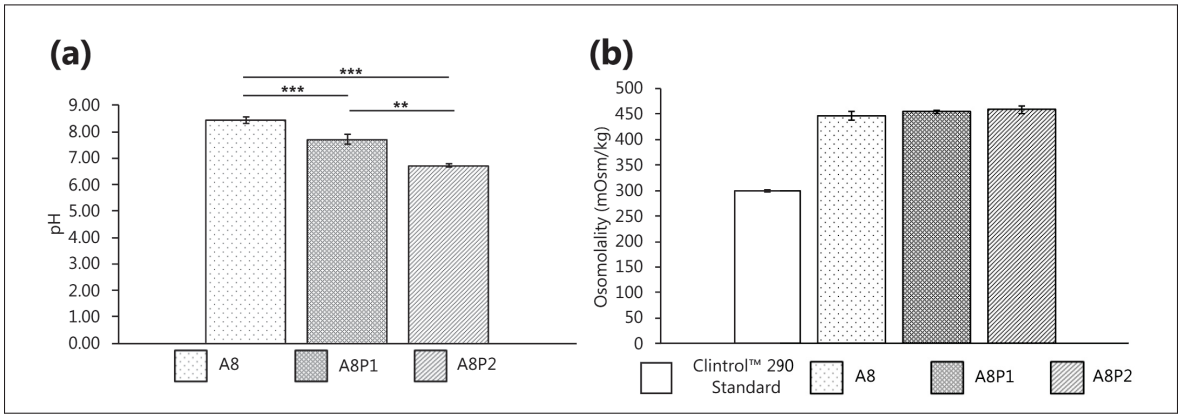

Figure 2.7 Physiochemical characterization of the foams (a) pH measurements of each foam composition. (mean +/- SD, $n = 3$, $*p < 0.05$, $**p < 0.01$, $***p < 0.001$) (b) Osmolality measurements of the liquid solutions for each foam composition prior to foaming. For osmolality measurements, no significant pairwise differences were detected between the 3 foam conditions presented (Tukey HSD, all $p \geq 0.05$)

2.4.6 Chitosan Microstructure Characterization

As shown in Figure 8, the foam support bath had some influence on the microstructure of the chitosan hydrogels, especially at their surface. Constructs printed into the A8P1 foam exhibited a visibly more porous structure compared to identical chitosan hydrogels printed directly on a surface without foam. In lyophilized foam-printed samples, SEM images (Figure 2.8(a)) revealed larger and more interconnected pores, while controls produced compact, dense microstructures with minimal internal voids. Histological analysis (Figure 2.8(b)) also showed a rough and irregular boundary in foam-printed hydrogels, with small air-derived cavities embedded along the interface, in contrast to the smooth, continuous border observed in controls. These differences likely arise from two coupled mechanisms. First, air bubbles in the foam indent the surface of the extruded chitosan before gelation and may become transiently trapped as the hydrogel solidifies, leading to the formation of surface and internal voids. Second, electrostatic interactions between the positively charged chitosan precursor and the negatively charged albumin–pectin complexes at the foam air–liquid interface create localized adhesion points that deform the hydrogel as it gels. Protein–polysaccharide complexes such as albumin–pectin are known to adsorb strongly at bubble surfaces, increasing interfacial elasticity and modifying local microstructure; similar templating effects have been reported in food foams and in bioprinting with granular support baths, where the microstructure of printed hydrogels correlates with the size or packing of surrounding microparticles (Schmidt *et al.*, 2010; Sadahira *et al.*, 2015; Brunel *et al.*, 2024). These observations align with previous findings showing that support bath composition and structural features can modulate pore morphology in collagen and other bioinks (Brunel *et al.*, 2024). The authors concluded that porosity is governed by the ratio between the shear viscosity of the ink and the zero-shear viscosity of the microgel support bath. Here, the strong viscosity of the bioink limits more or less this effect to the surface of the filament. Taken together, these results demonstrate that in-foam bioprinting not only stabilizes soft hydrogels mechanically but also serves as a microstructural templating environment, offering a simple means to modulate porosity.

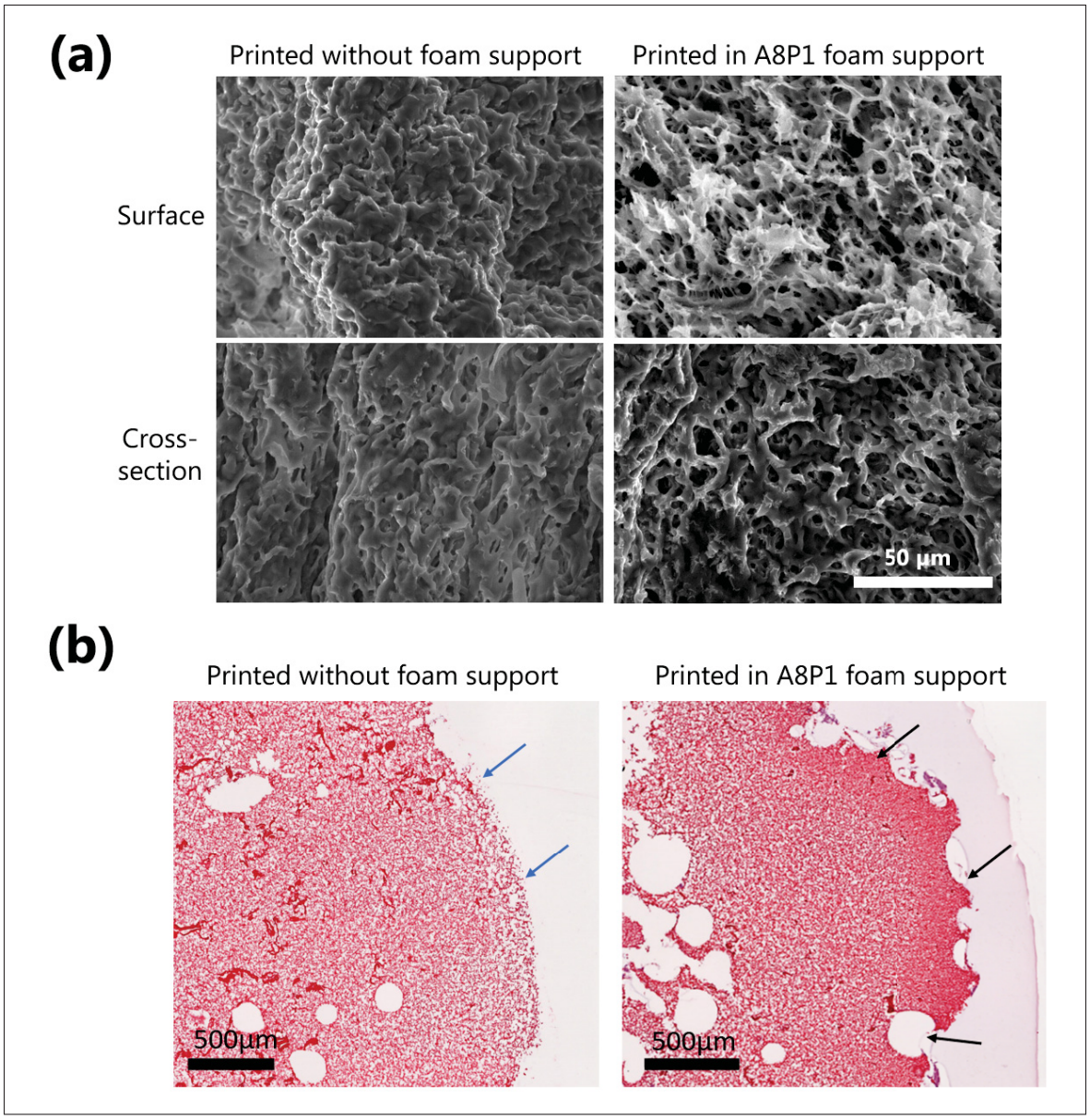

Figure 2.8 Microstructure characterization of the chitosan hydrogel used in the printability and cell viability studies (a) SEM imaging of the surface and cross-section of a chitosan structures printed either without a foam support (left) or inside an A8P1 foam support (right) (b) histology of chitosan hydrogel printed either with or without an A8P1 foam support

Despite these promising findings, in-foam bioprinting still presents several limitations. A key practical challenge is the opacity of the foam, which makes it difficult to visually monitor the extrusion of bioink during printing. This can hinder the detection of issues such as nozzle

clogging, irregular flow, or printing defects in real time. The lack of transparency also restricts the use of bioinks that require photopolymerization crosslinking, such as gelatin methacryloyl (GelMA) (Kumar *et al.*, 2021a), poly(ethylene glycol) (PEG) (Acosta-Vélez, Zhu, Linsley & Wu, 2018), and some modified hyaluronic acid (HA)-derived hydrogels (Ghorbani *et al.*, 2023), since light cannot penetrate efficiently through the foam.

Looking forward, there are several avenues for optimization. The present work focused on foams prepared from chicken egg white albumin, but future efforts could investigate human-derived albumin to improve translational potential, particularly for fabricating transplantable tissues or patient-specific disease models. Alternative foaming agents beyond albumin also remain unexplored and may broaden the range of compatible bioinks. In addition, the use of other polysaccharide stabilizers may further extend foam stability and printing windows. Together, these directions offer pathways to expand the versatility and clinical relevance of in-foam bioprinting.

2.5 Conclusions

This study demonstrates that incorporating pectin into albumin-based foams significantly improves their stability and performance as support baths for embedded bioprinting. The addition of pectin delayed liquid drainage, reduced bubble coalescence, and narrowed bubble size distributions, while preserving the essential rheological properties of shear-thinning behavior and rapid recovery after deformation. These physicochemical improvements enabled the successful printing of chitosan, a low-viscosity and slow-crosslinking hydrogel, into complex freeform structures with high fidelity. Importantly, the stabilized foams maintained cell viability during and after printing, outperforming conventional gelatin-based FRESH supports, particularly over extended incubation times, due to enhanced oxygen diffusion and a more favorable pH microenvironment.

Together, these results highlight albumin–pectin foams as a promising new class of support materials that combine mechanical support, nutrient permeability, and biological compatibility.

By addressing longstanding challenges in embedded bioprinting, this work expands the palette of printable bioinks and opens new opportunities for fabricating functional tissue constructs. Future work should focus on translating this platform toward clinical applications by exploring human-derived albumin, alternative stabilizers, and strategies for incorporating bioinks requiring photopolymerization.

2.6 Acknowledgements

This research was funded by the National Sciences and Research Council of Canada (Discovery Grant RGPIN-2023-05684 (AA) and RGPIN 2020-06684 (SL)) and Canada Foundation for Innovation (John R. Evans Leader Fund 37696). Natural Sciences and Engineering Research Council of Canada (NSERC) Canadian Graduate Scholarship – Master's (CGS M)

CONCLUSION AND RECOMMENDATIONS

The work presented in this thesis demonstrates that incorporating pectin into albumin-based foams enhances their performance as support baths for embedded bioprinting. By improving stability through delayed liquid drainage, slowed bubble coalescence, and narrower bubble size distributions, while maintaining shear-thinning and rapid recovery properties, pectin-stabilized foams overcome a central limitation of albumin-only formulations. These improvements enabled the successful printing of chitosan, a challenging low-viscosity and slow-crosslinking hydrogel, into multilayered freeform structures with high fidelity. Further, pectin-stabilized albumin foams supported high cell viability throughout printing and incubation, outperforming conventional gelatin microparticle FRESH baths, which can limit oxygen and nutrient availability over long durations. The enhanced dissolved oxygen levels and favorable pH environment provided by albumin–pectin foams likely contributed to this improved biological performance.

Taken together, these findings establish albumin–pectin foams as a promising new class of support materials that uniquely combine easy preparation and removal steps with mechanical stability, oxygen and nutrient permeability, and biocompatibility. This approach broadens the the palette of printable bioinks and expands the potential for fabricating functional complex tissue constructs that are not attainable with currently existing technologies by addressing longstanding challenges in embedded bioprinting. Looking forward, translation of this platform could be advanced by evaluating human-derived albumin as the foaming agent and printing human derived cells within it. Further, it is worth exploring alternative foaming agents and polysaccharide stabilizers. Another recommendation moving forward with in-foam bioprinting is to investigate integrating bioinks requiring photopolymerization. Ultimately, the development of oxygen-permeable, self-removable, and biologically relevant foams provides a step toward reliable, scalable, and clinically translatable embedded bioprinting strategies. A strategy that will help support the creation of physiologically relevant tissue and disease models, accelerate

the testing of therapeutic interventions, and, in the long term, bring the field closer to one day bioprinting functional, patient-specific organs to help address the global organ shortage.

APPENDIX I

STERILIZATION METHODS

Table A I-1 outlines how each material was sterilized during the cell based studies. Sterilization was required in order to prevent contamination by unwanted microorganisms (e.g. bacteria, fungi, etc.).

Table-A I-1 Sterilization techniques for materials in cell-based tests

Material	**Sterilization Technique**
Pectin powder	30 minute UV exposure
Albumin powder	30 minute UV exposure
Gelatin powder	30 minute UV exposure
Chitosan hydrogel	Autoclave (121°C for 20 minutes)
Gelling agent solution (βGP + SHC)	Filtration using a 0.22 μm pore size syringe filter
PBS 1X	Autoclave (121°C for 20 minutes)
Print needles	Autoclave (121°C for 20 minutes)
Blender + Blender Blade	3 hour soak in 70% EtOH and 30 minute exposure to UV light
Tools (tweezers, luer locks, spatulas, beakers, magnetic stir bars, overhead stirrer blade, etc.)	Autoclave (121°C for 20 minutes)
O_2 planar sensors spots	Overnight soak in 100% EtOH

APPENDIX II

ADDITIONAL PH AND OSMOLALITY MEASUREMENTS

The pH and osmolality of several different components of each foam composition were measured. The pH and osmolality of the liquid solution prior to mechanically foaming the foams was measured. In addition, the pH and osmolality of the liquid drainage from each foam sample was collected and measured. It was important to take measurements of the liquid drainage since as the foam breaks down the cells at the bottom of the printed structure could be in contact with the liquid that has drained down from the foam. Lastly, the pH of the foamed foam was measured. However, the osmolality of the foam itself was not measured, since the osmometer used is only compatible with small liquid samples. To make the graph easier to read, not all measurements were reported in Figure 2.7 in section 2.4.5 of the thesis and are instead listed below in Figures-A II-1 and II-2.

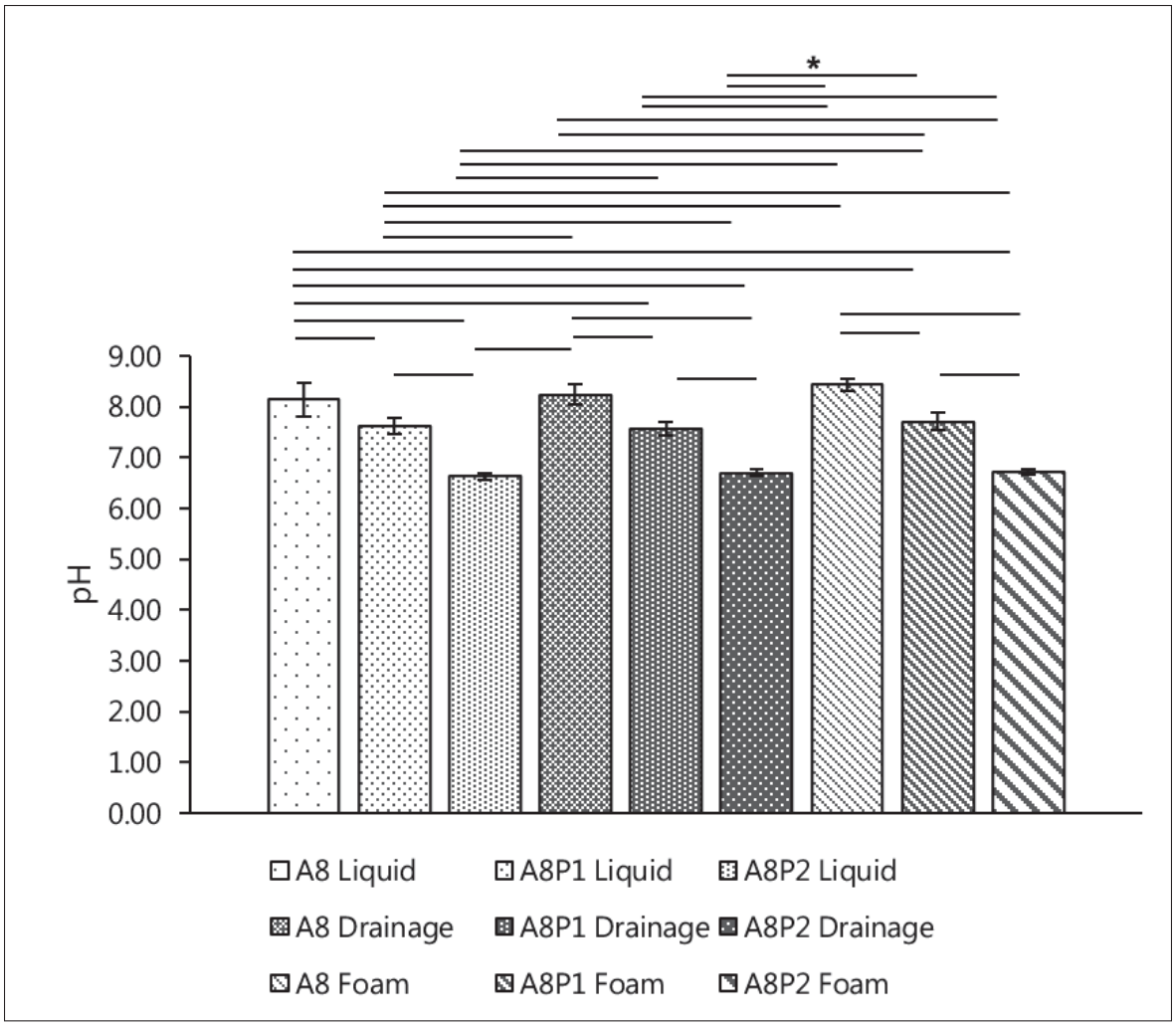

Figure-A II-1 pH values of various components of the foams prepared including the liquid before foaming, the foams itself and the liquid drainage from the foam (mean +/- SD, $n = 3$, $*p < 0.05$)

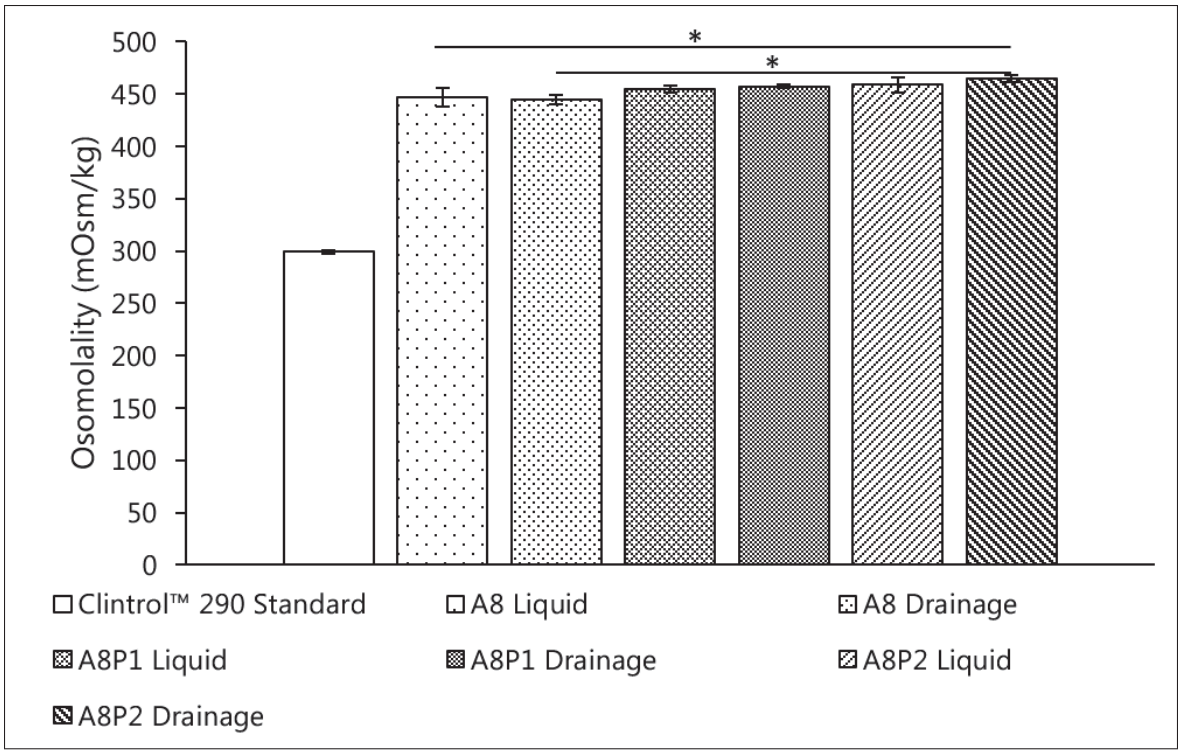

Figure-A II-2 pH values of various components of the foams prepared including the liquid before foaming, the foams itself and the liquid drainage from the foam (mean +/- SD, $n = 3$, $^*p < 0.05$)

APPENDIX III

FOAM SALINITY MEASUREMENTS

The salinity of the foams was measured in order to take accurate dissolved oxygen measurements and are reported in Table-A III-I.

Table-A III-1 Salinity of Foam and FRESH Support Baths

Support Bath	Salinity (ppt)	+/- Standard Deviation (ppt)
A8	0.6	0.2
A8P1	1.0	0.1
A8P2	1.4	0.1
DMEM FRESH	7.2	0.1
PBS FRESH	7.9	0.1

The PreSens sensor detects oxygen partial pressure (pO_2) via dynamic luminescence quenching by molecular oxygen (GmbH, 2025). The polymer optical fiber flashes excitation light from the instrument to the O_2 planar sensor spots and collecs the resulting luminescence signal. The sensor contains an immobilized luminophore whose excited state is quenched by molecular oxygen through dynamic quenching. This interaction shortens the luminescence lifetime in proportion to the local oxygen concentration. Salinity was measured to correct for its effect on oxygen solubility during the conversion of oxygen partial pressure into dissolved oxygen concentration. According to Henry's law, the solubility of gases is proportional to their partial pressure; however, the presence of salts reduces oxygen solubility through a salting-out effect (Langmuir, 1997). Including salinity as a parameter allowed accurate conversion of oxygen partial pressure, measured optically, into dissolved oxygen concentration (see equation A IV-1) (Zumdahl & Zumdahl, 2000).

$$[O_2] = \alpha \cdot pO_2 \qquad \text{(A III-1)}$$

where $[O_2]$ is the concentration of dissolved oxygen in the sample, α a proportionality factor dependent on the solutions salinity and temperature, and pO_2 is the partial pressure of the the oxygen.

APPENDIX IV

ADDITIONAL PRINTABILITY PHOTOS

Below are images demonstrating how the printed constructs were removed from the foam support bath. Further, additional images taken to investigate the printability of 2% chitosan hydrogels in each of the foam compositions studied (A8, A8P1, A8P2) are presented.

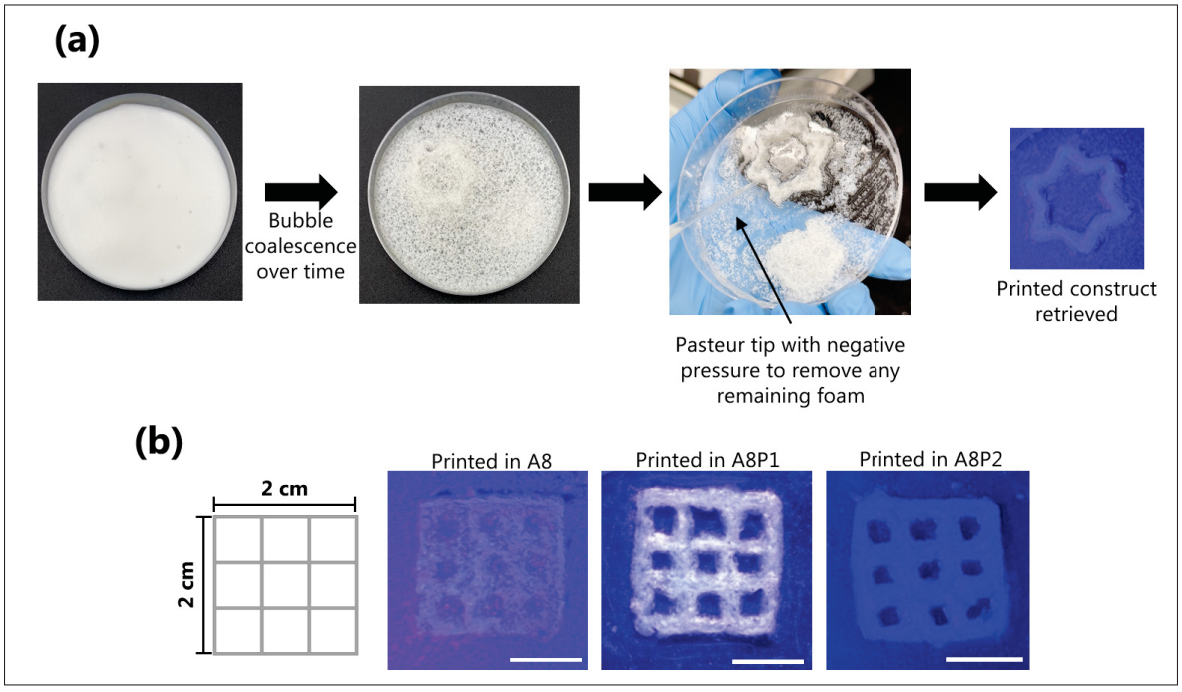

Figure-A IV-1 (a) Support bath removal. The bubbles coaslece naturally over time, afterwhich any excess foam can be removed using a Pasteur tip and negative pressure (b) 2 x 2 cm grids printed in each of the foam supports studies (A8, A8P1, A8P2). Scale bars are 1 cm

BIBLIOGRAPHY

Abeyrathne, E. N. S., Lee, H. & Ahn, D. U. (2013). Egg white proteins and their potential use in food processing or as nutraceutical and pharmaceutical agents—A review. *Poultry science*, 92(12), 3292–3299.

Acosta-Vélez, G. F., Zhu, T. Z., Linsley, C. S. & Wu, B. M. (2018). Photocurable poly (ethylene glycol) as a bioink for the inkjet 3D pharming of hydrophobic drugs. *International journal of pharmaceutics*, 546(1-2), 145–153.

Afghah, F., Altunbek, M., Dikyol, C. & Koc, B. (2020). Preparation and characterization of nanoclay-hydrogel composite support-bath for bioprinting of complex structures. *Scientific reports*, 10(1), 5257.

Agarwal, K., Srinivasan, V., Lather, V., Pandita, D. & Vasanthan, K. S. (2023). Insights of 3D bioprinting and focusing the paradigm shift towards 4D printing for biomedical applications. *Journal of Materials Research*, 38(1), 112–141.

Alinejad, Y., Adoungotchodo, A., Grant, M. P., Epure, L. M., Antoniou, J., Mwale, F. & Lerouge, S. (2019). Injectable chitosan hydrogels with enhanced mechanical properties for nucleus pulposus regeneration. *Tissue Engineering Part A*, 25(5-6), 303–313.

Allevi. [Company protocol page]. (2020). FRESH Bioprinting Using LifeSupport Protocol. Retrieved on 2025-09-25 from: https://www.allevi3d.com/fresh-bioprinting-using-lifesupport-protocol/.

Almouemen, N., Kelly, H. M. & O'leary, C. (2019). Tissue engineering: understanding the role of biomaterials and biophysical forces on cell functionality through computational and structural biotechnology analytical methods. *Computational and structural biotechnology journal*, 17, 591–598.

Amante, C., Andretto, V., Rosso, A., Augusti, G., Marzocco, S., Lollo, G. & Del Gaudio, P. (2023). Alginate-pectin microparticles loaded with nanoemulsions as nanocomposites for wound healing. *Drug Delivery and Translational Research*, 13(5), 1343–1357.

Arenholt-Bindslev, D., Bleeg, H. S. & Richards, A. (1992). Toxicity of sodium dodecyl sulphate and other detergents in cultures of human oral mucosa epithelium. *Alternatives to Laboratory Animals*, 20(1), 28–38.

Armstrong, J. P. & Stevens, M. M. (2019). Emerging technologies for tissue engineering: from gene editing to personalized medicine. *Tissue Engineering Part A*, 25(9-10), 688–692.

Assaad, E., Maire, M. & Lerouge, S. (2015). Injectable thermosensitive chitosan hydrogels with controlled gelation kinetics and enhanced mechanical resistance. *Carbohydrate polymers*, 130, 87–96.

Atala, A. & Lanza, R. (2002). *Methods of tissue engineering*. Gulf professional publishing.

Axpe, E. & Oyen, M. L. (2016). Applications of alginate-based bioinks in 3D bioprinting. *International journal of molecular sciences*, 17(12), 1976.

Babu, S., Shanmugavadivu, A. & Selvamurugan, N. (2024). Tunable mechanical properties of chitosan-based biocomposite scaffolds for bone tissue engineering applications: a review. *International Journal of Biological Macromolecules*, 272, 132820.

Badr, S., Madadian, E., MacDonald, D., Tasker, R. A. & Ahmadi, A. (2023). A mist-based crosslinking technique for coaxial bioprinting of hollow hydrogel fibers. *Bioprinting*, 35, e00308.

Badylak, S. F., Taylor, D. & Uygun, K. (2011). Whole-organ tissue engineering: decellularization and recellularization of three-dimensional matrix scaffolds. *Annual review of biomedical engineering*, 13(1), 27–53.

Bajpai, A. & Saini, R. (2006). Preparation and characterization of novel biocompatible cryogels of poly (vinyl alcohol) and egg-albumin and their water sorption study. *Journal of Materials Science: Materials in Medicine*, 17(1), 49–61.

Bao, G., Jiang, T., Ravanbakhsh, H., Reyes, A., Ma, Z., Strong, M., Wang, H., Kinsella, J. M., Li, J. & Mongeau, L. (2020). Triggered micropore-forming bioprinting of porous viscoelastic hydrogels. *Materials horizons*, 7(9), 2336–2347.

Basu, A., Saha, A., Goodman, C., Shafranek, R. T. & Nelson, A. (2017). Catalytically initiated gel-in-gel printing of composite hydrogels. *ACS applied materials & interfaces*, 9(46), 40898–40904.

Bessler, N., Ogiermann, D., Buchholz, M.-B., Santel, A., Heidenreich, J., Ahmmed, R., Zaehres, H. & Brand-Saberi, B. (2019). Nydus One Syringe Extruder (NOSE): A Prusa i3 3D printer conversion for bioprinting applications utilizing the FRESH-method. *HardwareX*, 6, e00069.

Betancourt, N. & Chen, X. (2022). Review of extrusion-based multi-material bioprinting processes. *Bioprinting*, 25, e00189.

Bhattacharjee, T., Zehnder, S. M., Rowe, K. G., Jain, S., Nixon, R. M., Sawyer, W. G. & Angelini, T. E. (2015). Writing in the granular gel medium. *Science advances*, 1(8), e1500655.

Bishop, E. S., Mostafa, S., Pakvasa, M., Luu, H. H., Lee, M. J., Wolf, J. M., Ameer, G. A., He, T.-C. & Reid, R. R. (2017). 3-D bioprinting technologies in tissue engineering and regenerative medicine: Current and future trends. *Genes & diseases*, 4(4), 185–195.

Bordoni, M., Karabulut, E., Kuzmenko, V., Fantini, V., Pansarasa, O., Cereda, C. & Gatenholm, P. (2020). 3D printed conductive nanocellulose scaffolds for the differentiation of human neuroblastoma cells. *Cells*, 9(3), 682.

Bostancı, N. S., Büyüksungur, S., Hasirci, N. & Tezcaner, A. (2022). Potential of pectin for biomedical applications: A comprehensive review. *Journal of Biomaterials Science, Polymer Edition*, 33(14), 1866–1900.

Bouyer, E., Mekhloufi, G., Rosilio, V., Grossiord, J.-L. & Agnely, F. (2012). Proteins, polysaccharides, and their complexes used as stabilizers for emulsions: Alternatives to synthetic surfactants in the pharmaceutical field? *International journal of pharmaceutics*, 436(1-2), 359–378.

Brown, N., de la Pena, A. & Razavi, S. (2023). Interfacial rheology insights: particle texture and Pickering foam stability. *Journal of Physics: Condensed Matter*, 35(38), 384002.

Brunel, L. G., Hull, S. M. & Heilshorn, S. C. (2022). Engineered assistive materials for 3D bioprinting: support baths and sacrificial inks. *Biofabrication*, 14(3), 032001.

Brunel, L. G., Christakopoulos, F., Kilian, D., Cai, B., Hull, S. M., Myung, D. & Heilshorn, S. C. (2024). Embedded 3D bioprinting of collagen inks into microgel baths to control hydrogel microstructure and cell spreading. *Advanced healthcare materials*, 13(25), 2303325.

Budharaju, H., Sundaramurthi, D. & Sethuraman, S. (2024). Embedded 3D bioprinting–An emerging strategy to fabricate biomimetic & large vascularized tissue constructs. *Bioactive Materials*, 32, 356–384.

Caiado Decarli, M., Ferreira, H. P., Sobreiro-Almeida, R., Teixeira, F. C., Correia, T. R., Babilotte, J., Olijve, J., Custódio, C. A., Gonçalves, I. C., Mota, C. et al. (2025). Embedding Bioprinting of Low Viscous, Photopolymerizable Blood-Based Bioinks in a Crystal Self-Healing Transparent Supporting Bath. *Small methods*, 9(1), 2400857.

Cao, H., Duan, L., Zhang, Y., Cao, J. & Zhang, K. (2021). Current hydrogel advances in physicochemical and biological response-driven biomedical application diversity. *Signal transduction and targeted therapy*, 6(1), 426.

Catori, D. M., Lorevice, M. V., da Silva, L. C., Candido, G., Millás, A. L. & de Oliveira, M. G. (2022). Fresh 3D Printing of Double Crosslinked Hyaluronic Acid/Pectin Hydrogels. *Macromolecular Symposia*, 406(1), 2200050.

Ceccaldi, C., Assaad, E., Hui, E., Buccionyte, M., Adoungotchodo, A. & Lerouge, S. (2017). Optimization of injectable thermosensitive scaffolds with enhanced mechanical properties for cell therapy. *Macromolecular bioscience*, 17(6), 1600435.

Chang, J. & Sun, X. (2023). Laser-induced forward transfer based laser bioprinting in biomedical applications. *Frontiers in Bioengineering and Biotechnology*, 11, 1255782.

Chen, W. W., Tjin, M. S., Chua, A. W., Lee, S. T., Tay, C. Y. & Fong, E. (2017). Probing the role of integrins in keratinocyte migration using bioengineered extracellular matrix mimics. *ACS applied materials & interfaces*, 9(42), 36483–36492.

Choi, Y.-J., Jun, Y.-J., Kim, D. Y., Yi, H.-G., Chae, S.-H., Kang, J., Lee, J., Gao, G., Kong, J.-S., Jang, J. et al. (2019). A 3D cell printed muscle construct with tissue-derived bioink for the treatment of volumetric muscle loss. *Biomaterials*, 206, 160–169.

Choudhury, D., Anand, S. & Naing, M. W. (2018). The arrival of commercial bioprinters–towards 3D bioprinting revolution! *International Journal of Bioprinting*, 4(2), 139.

Chung, B. G., Lee, K.-H., Khademhosseini, A. & Lee, S.-H. (2012). Microfluidic fabrication of microengineered hydrogels and their application in tissue engineering. *Lab on a Chip*, 12(1), 45–59.

Cidonio, G., Cooke, M., Glinka, M., Dawson, J., Grover, L. & Oreffo, R. (2019). Printing bone in a gel: using nanocomposite bioink to print functionalised bone scaffolds. *Materials Today Bio*, 4, 100028.

Compaan, A. M., Song, K. & Huang, Y. (2019). Gellan fluid gel as a versatile support bath material for fluid extrusion bioprinting. *ACS applied materials & interfaces*, 11(6), 5714–5726.

Compaan, A. M., Song, K., Chai, W. & Huang, Y. (2020). Cross-linkable microgel composite matrix bath for embedded bioprinting of perfusable tissue constructs and sculpting of solid objects. *ACS Applied Materials & Interfaces*, 12(7), 7855–7868.

Cooke, M. E., Riffe, M. B., Gomes, M. E., Domingues, R. M. & Burdick, J. A. (2025). Biofabrication in suspension media—a decade of advances. *Biofabrication*, 17(3), 033001.

Courbot, O. & Elosegui-Artola, A. (2025). The role of extracellular matrix viscoelasticity in development and disease. *npj Biological Physics and Mechanics*, 2(1), 10.

Cui, X., Boland, T., DD'Lima, D. & K. Lotz, M. (2012). Thermal inkjet printing in tissue engineering and regenerative medicine. *Recent patents on drug delivery & formulation*, 6(2), 149–155.

Daly, A. C., Davidson, M. D. & Burdick, J. A. (2021). 3D bioprinting of high cell-density heterogeneous tissue models through spheroid fusion within self-healing hydrogels. *Nature communications*, 12(1), 753.

Damodaran, S. (2005). Protein stabilization of emulsions and foams. *Journal of food science*, 70(3), R54–R66.

De Graav, G. N., Udomkarnjananun, S., Baan, C. C., Reinders, M. E., Roodnat, J. I., De Winter, B. C. & Hesselink, D. A. (2025). New developments and therapeutic drug monitoring options in costimulatory blockade in solid organ transplantation: a systematic critical review. *Therapeutic drug monitoring*, 47(1), 64–76.

de Melo, B. A., Jodat, Y. A., Cruz, E. M., Benincasa, J. C., Shin, S. R. & Porcionatto, M. A. (2020). Strategies to use fibrinogen as bioink for 3D bioprinting fibrin-based soft and hard tissues. *Acta biomaterialia*, 117, 60–76.

Delaporte, P. & Alloncle, A.-P. (2016). Laser-induced forward transfer: A high resolution additive manufacturing technology. *Optics & Laser Technology*, 78, 33–41.

Deng, Z., Wang, T., Chen, X. & Liu, Y. (2020). Applications of chitosan-based biomaterials: a focus on dependent antimicrobial properties. *Marine Life Science & Technology*, 2(4), 398–413.

Derakhshanfar, S., Mbeleck, R., Xu, K., Zhang, X., Zhong, W. & Xing, M. (2018). 3D bioprinting for biomedical devices and tissue engineering: A review of recent trends and advances. *Bioactive materials*, 3(2), 144–156.

Derman, I. D., Kim, M. H., Sarikaya, M. D., Yilmaz, Y. O., Aliftiras, E. G., Stepanyants, V., Rivera, T. & Ozbolat, I. T. (2025). Unconventional Bioprinting Modalities for Advanced Tissue Biofabrication. *Biomaterials*, 123704.

Dickinson, E. (2010). Food emulsions and foams: Stabilization by particles. *Current Opinion in Colloid & Interface Science*, 15(1-2), 40–49.

Ding, H. & Chang, R. C. (2018). Printability study of bioprinted tubular structures using liquid hydrogel precursors in a support bath. *Applied Sciences*, 8(3), 403.

Dou, C., Perez, V., Qu, J., Tsin, A., Xu, B. & Li, J. (2021). A state-of-the-art review of laser-assisted bioprinting and its future research trends. *ChemBioEng Reviews*, 8(5), 517–534.

Duan, X., Li, M., Shao, J., Chen, H., Xu, X., Jin, Z. & Liu, X. (2018). Effect of oxidative modification on structural and foaming properties of egg white protein. *Food Hydrocolloids*, 75, 223–228.

Eivazzadeh-Keihan, R., Pourakbari, B., Jahani, Z., Aliabadi, H. A. M., Kashtiaray, A., Rahmati, S., Pouri, S., Ghafuri, H., Maleki, A. & Mahdavi, M. (2022). Biological investigation of a novel nanocomposite based on functionalized graphene oxide nanosheets with pectin, silk fibroin and zinc chromite nanoparticles. *Journal of Biotechnology*, 358, 55–63.

Eltom, A., Zhong, G. & Muhammad, A. (2019). Scaffold techniques and designs in tissue engineering functions and purposes: a review. *Advances in materials science and engineering*, 2019(1), 3429527.

Fang, Y., Guo, Y., Wu, B., Liu, Z., Ye, M., Xu, Y., Ji, M., Chen, L., Lu, B., Nie, K. et al. (2023). Expanding embedded 3D bioprinting capability for engineering complex organs with freeform vascular networks. *Advanced Materials*, 35(22), 2205082.

Gharbi, N. & Labbafi, M. (2019). Influence of treatment-induced modification of egg white proteins on foaming properties. *Food hydrocolloids*, 90, 72–81.

Ghorbani, F., Ghalandari, B., Khajehmohammadi, M., Bakhtiary, N., Tolabi, H., Sahranavard, M., Fathi-Karkan, S., Nazar, V., Hasan Niari Niar, S., Armoon, A. et al. (2023). Photo-cross-linkable hyaluronic acid bioinks for bone and cartilage tissue engineering applications. *International Materials Reviews*, 68(7), 901–942.

GmbH, P. P. S. (2025). Measurement principle of chemical optical sensors. *PreSens Knowledge Base*. Retrieved from: https://www.presens.de/knowledge/basics/detail/measurement-principle-of-chemical-optical-sensors-901.

Gong, C., Kong, Z. & Wang, X. (2021). The effect of agarose on 3D bioprinting. *Polymers*, 13(22), 4028.

Grant, G. T., Morris, E. R., Rees, D. A., Smith, P. J. & Thom, D. (1973). Biological interactions between polysaccharides and divalent cations: the egg-box model. *FEBS letters*, 32(1), 195–198.

Guha, S., Majumder, K. & Mine, Y. (2019). Encyclopedia of food chemistry. Elsevier Amsterdam, The Netherlands:.

Guler, S., Aslan, B., Hosseinian, P. & Aydin, H. M. (2017). Supercritical carbon dioxide-assisted decellularization of aorta and cornea. *Tissue Engineering Part C: Methods*, 23(9), 540–547.

Gungor-Ozkerim, P. S., Inci, I., Zhang, Y. S., Khademhosseini, A. & Dokmeci, M. R. (2018). Bioinks for 3D bioprinting: an overview. *Biomaterials science*, 6(5), 915–946.

Gunnink, S. M., Kerk, S. A., Kuiper, B. D., Alabi, O. D., Kuipers, D. P., Praamsma, R. C., Wrobel, K. E. & Louters, L. L. (2014). Alkaline pH activates the transport activity of GLUT1 in L929 fibroblast cells. *Biochimie*, 99, 189–194.

Han, F., Wang, J., Ding, L., Hu, Y., Li, W., Yuan, Z., Guo, Q., Zhu, C., Yu, L., Wang, H. et al. (2020). Tissue engineering and regenerative medicine: achievements, future, and sustainability in Asia. *Frontiers in bioengineering and biotechnology*, 8, 83.

Han, Y., Zhu, L., Zhang, H. & Liu, T. (2024). Mechanism of sucrose improving the mechanical characteristics of foams stabilized by soy protein isolate/gellan gum/guar gum ternary complex. *International Journal of Biological Macromolecules*, 280, 135845.

Highley, C. B., Rodell, C. B. & Burdick, J. A. (2015). Direct 3D Printing of Shear-Thinning Hydrogels into Self-Healing Hydrogels. *Advanced Materials (Deerfield Beach, Fla.)*, 27(34), 5075–5079.

Hinton, T. J., Jallerat, Q., Palchesko, R. N., Park, J. H., Grodzicki, M. S., Shue, H.-J., Ramadan, M. H., Hudson, A. R. & Feinberg, A. W. (2015). Three-dimensional printing of complex biological structures by freeform reversible embedding of suspended hydrogels. *Science advances*, 1(9), e1500758.

Hinton, T. J., Hudson, A., Pusch, K., Lee, A. & Feinberg, A. W. (2016). 3D printing PDMS elastomer in a hydrophilic support bath via freeform reversible embedding. *ACS biomaterials science & engineering*, 2(10), 1781–1786.

Hoang, V. T., Nguyen, Q. T., Phan, T. T. K., Pham, T. H., Dinh, N. T. H., Anh, L. P. H., Dao, L. T. M., Bui, V. D., Dao, H.-N., Le, D. S. et al. (2025). Tissue Engineering and Regenerative Medicine: Perspectives and Challenges. *MedComm*, 6(5), e70192.

Hopkins, E., Sanvictores, T. & Sharma, S. (2018). Physiology, acid base balance.

Hu, T., Cai, Z., Yin, R., Zhang, W., Bao, C., Zhu, L. & Zhang, H. (2023). 3D embedded printing of complex biological structures with supporting bath of pluronic F-127. *Polymers*, 15(17), 3493.

Hua, W., Mitchell, K., Raymond, L., Godina, B., Zhao, D., Zhou, W. & Jin, Y. (2021). Fluid bath-assisted 3D printing for biomedical applications: from pre-to postprinting stages. *ACS biomaterials science & engineering*, 7(10), 4736–4756.

Huh, D., Hamilton, G. A. & Ingber, D. E. (2011). From 3D cell culture to organs-on-chips. *Trends in cell biology*, 21(12), 745–754.

Hull, S. M., Lou, J., Lindsay, C. D., Navarro, R. S., Cai, B., Brunel, L. G., Westerfield, A. D., Xia, Y. & Heilshorn, S. C. (2023). 3D bioprinting of dynamic hydrogel bioinks enabled by small molecule modulators. *Science Advances*, 9(13), eade7880.

Ince Coşkun, A. E. & Özdestan Ocak, Ö. (2021). Foaming properties of different forms of caseins in aqueous systems. *Journal of Food Measurement and Characterization*, 15(3), 2275–2284.

Jeon, O., Lee, Y. B., Jeong, H., Lee, S. J., Wells, D. & Alsberg, E. (2019). Individual cell-only bioink and photocurable supporting medium for 3D printing and generation of engineered tissues with complex geometries. *Materials horizons*, 6(8), 1625–1631.

Ji, S. & Guvendiren, M. (2017). Recent advances in bioink design for 3D bioprinting of tissues and organs. *Frontiers in bioengineering and biotechnology*, 5, 23.

Jiménez-Gómez, C. P. & Cecilia, J. A. (2020). Chitosan: a natural biopolymer with a wide and varied range of applications. *Molecules*, 25(17), 3981.

Jin, Y., Compaan, A., Bhattacharjee, T. & Huang, Y. (2016). Granular gel support-enabled extrusion of three-dimensional alginate and cellular structures. *Biofabrication*, 8(2), 025016.

Jin, Y., Chai, W. & Huang, Y. (2017). Printability study of hydrogel solution extrusion in nanoclay yield-stress bath during printing-then-gelation biofabrication. *Materials Science and Engineering: C*, 80, 313–325.

Jin, Y., Xiong, R., Antonelli, P. J., Long, C. J., McAleer, C. W., Hickman, J. J. & Huang, Y. (2021). Nanoclay suspension-enabled extrusion bioprinting of three-dimensional soft structures. *Journal of Manufacturing Science and Engineering*, 143(12), 121004.

Kačarević, Ž. P., Rider, P. M., Alkildani, S., Retnasingh, S., Smeets, R., Jung, O., Ivanišević, Z. & Barbeck, M. (2018). An introduction to 3D bioprinting: possibilities, challenges and future aspects. *Materials*, 11(11), 2199.

Karamchand, L., Makeiff, D., Gao, Y., Azyat, K., Serpe, M. J. & Kulka, M. (2023). Biomaterial inks and bioinks for fabricating 3D biomimetic lung tissue: A delicate balancing act between biocompatibility and mechanical printability. *Bioprinting*, 29, e00255.

Karoyo, A. H. & Wilson, L. D. (2021). A review on the design and hydration properties of natural polymer-based hydrogels. *Materials*, 14(5), 1095.

Karsa, D. R. & Houston, J. (2006). What are surfactants. *Chemistry and technology of surfactants*, 1.

Khoeini, R., Nosrati, H., Akbarzadeh, A., Eftekhari, A., Kavetskyy, T., Khalilov, R., Ahmadian, E., Nasibova, A., Datta, P., Roshangar, L. et al. (2021). Natural and synthetic bioinks for 3D bioprinting. *Advanced NanoBiomed Research*, 1(8), 2000097.

Kim, Y. S., Majid, M., Melchiorri, A. J. & Mikos, A. G. (2019). Applications of decellularized extracellular matrix in bone and cartilage tissue engineering. *Bioengineering & translational medicine*, 4(1), 83–95.

Kjar, A., McFarland, B., Mecham, K., Harward, N. & Huang, Y. (2021). Engineering of tissue constructs using coaxial bioprinting. *Bioactive materials*, 6(2), 460–471.

Kobayashi, J., Kikuchi, A., Aoyagi, T. & Okano, T. (2019). Cell sheet tissue engineering: cell sheet preparation, harvesting/manipulation, and transplantation. *Journal of biomedical materials research Part A*, 107(5), 955–967.

Kort-Mascort, J., Flores-Torres, S., Peza-Chavez, O., Jang, J. H., Pardo, L. A., Tran, S. D. & Kinsella, J. (2023). Decellularized ECM hydrogels: prior use considerations, applications, and opportunities in tissue engineering and biofabrication. *Biomaterials science*, 11(2), 400–431.

Kruse, C. R., Singh, M., Targosinski, S., Sinha, I., Sørensen, J. A., Eriksson, E. & Nuutila, K. (2017). The effect of pH on cell viability, cell migration, cell proliferation, wound closure, and wound reepithelialization: In vitro and in vivo study. *Wound Repair and Regeneration*, 25(2), 260–269.

Kumar, A., Yadav, S., Pramanik, J., Sivamaruthi, B. S., Jayeoye, T. J., Prajapati, B. G. & Chaiyasut, C. (2023). Chitosan-based composites: Development and perspective in food preservation and biomedical applications. *Polymers*, 15(15), 3150.

Kumar, H., Sakthivel, K., Mohamed, M. G., Boras, E., Shin, S. R. & Kim, K. (2021a). Designing gelatin methacryloyl (GelMA)-based bioinks for visible light stereolithographic 3D biofabrication. *Macromolecular Bioscience*, 21(1), 2000317.

Kumar, P., Ebbens, S. & Zhao, X. (2021b). Inkjet printing of mammalian cells–Theory and applications. *Bioprinting*, 23, e00157.

Lai, G. & Meagher, L. (2024). Versatile xanthan gum-based support bath material compatible with multiple crosslinking mechanisms: rheological properties, printability, and cytocompatibility study. *Biofabrication*, 16(3), 035005.

Lai, Y., Xiao, X., Huang, Z., Duan, H., Yang, L., Yang, Y., Li, C. & Feng, L. (2024). Photocrosslinkable biomaterials for 3D bioprinting: mechanisms, recent advances, and future prospects. *International Journal of Molecular Sciences*, 25(23), 12567.

Lam, S., Velikov, K. P. & Velev, O. D. (2014). Pickering stabilization of foams and emulsions with particles of biological origin. *Current Opinion in Colloid & Interface Science*, 19(5), 490–500.

Lancaster, M. A. & Knoblich, J. A. (2014). Organogenesis in a dish: modeling development and disease using organoid technologies. *Science*, 345(6194), 1247125.

Langmuir, D. (1997). *Aqueous environmental geochemistry*. New Jersey.

Lee, A., Hudson, A., Shiwarski, D., Tashman, J., Hinton, T., Yerneni, S., Bliley, J., Campbell, P. & Feinberg, A. (2019). 3D bioprinting of collagen to rebuild components of the human heart. *Science*, 365(6452), 482–487.

Li, W., Wang, M., Ma, H., Chapa-Villarreal, F. A., Lobo, A. O. & Zhang, Y. S. (2023). Stereolithography apparatus and digital light processing-based 3D bioprinting for tissue fabrication. *Iscience*, 26(2).

Li, X., Liu, B., Pei, B., Chen, J., Zhou, D., Peng, J., Zhang, X., Jia, W. & Xu, T. (2020). Inkjet bioprinting of biomaterials. *Chemical reviews*, 120(19), 10793–10833.

Li, Z. & Kawashita, M. (2011). Current progress in inorganic artificial biomaterials. *Journal of Artificial Organs*, 14(3), 163–170.

Linke, D. & Berger, R. (2011). Foaming of proteins: new prospects for enzyme purification processes. *Journal of biotechnology*, 152(4), 125–131.

Lu, J., Gao, Z., He, W. & Lu, Y. (2025). Harnessing the potential of hyaluronic acid methacrylate (HAMA) hydrogel for clinical applications in orthopaedic diseases. *Journal of Orthopaedic Translation*, 50, 111–128.

Madadian, E., Naseri, E., Legault, R. & Ahmadi, A. (2024a). Development of 3D-printable albumin–alginate foam for wound dressing applications. *3D Printing and Additive Manufacturing*, 11(3), e1175–e1185.

Madadian, E., Ravanbakhsh, H., Touani Kameni, F., Rahimnejad, M., Lerouge, S. & Ahmadi, A. (2024b). In-Foam Bioprinting: An Embedded Bioprinting Technique with Self-Removable Support Bath. *Small Science*, 2300280.

Mancha Sánchez, E., Gómez-Blanco, J. C., López Nieto, E., Casado, J. G., Macías-García, A., Díaz Díez, M. A., Carrasco-Amador, J. P., Torrejón Martín, D., Sánchez-Margallo, F. M. & Pagador, J. B. (2020). Hydrogels for bioprinting: A systematic review of hydrogels synthesis, bioprinting parameters, and bioprinted structures behavior. *Frontiers in Bioengineering and Biotechnology*, 8, 776.

Mandrycky, C., Wang, Z., Kim, K. & Kim, D.-H. (2016). 3D bioprinting for engineering complex tissues. *Biotechnology advances*, 34(4), 422–434.

Maxson, E. L., Young, M. D., Noble, C., Go, J. L., Heidari, B., Khorramirouz, R., Morse, D. W. & Lerman, A. (2019). In vivo remodeling of a 3D-Bioprinted tissue engineered heart valve scaffold. *Bioprinting*, 16, e00059.

Méndez, D. A., Schröter, B., Martínez-Abad, A., Fabra, M. J., Gurikov, P. & López-Rubio, A. (2023). Pectin-based aerogel particles for drug delivery: Effect of pectin composition on aerogel structure and release properties. *Carbohydrate polymers*, 306, 120604.

Miquelim, J. N., Lannes, S. C. & Mezzenga, R. (2010). pH Influence on the stability of foams with protein–polysaccharide complexes at their interfaces. *Food hydrocolloids*, 24(4), 398–405.

Mirdamadi, E., Muselimyan, N., Koti, P., Asfour, H. & Sarvazyan, N. (2019). Agarose slurry as a support medium for bioprinting and culturing freestanding cell-laden hydrogel constructs. *3D printing and additive manufacturing*, 6(3), 158–164.

Mohanan, A., Nickerson, M. T. & Ghosh, S. (2020). Utilization of pulse protein-xanthan gum complexes for foam stabilization: The effect of protein concentrate and isolate at various pH. *Food Chemistry*, 316, 126282.

Mooney, D. J. & Vacanti, J. P. (1993). Tissue engineering using cells and synthetic polymers. *Transplantation Reviews*, 7(3), 153–162.

Morello, G., De Iaco, G., Gigli, G., Polini, A. & Gervaso, F. (2023). Chitosan and pectin hydrogels for tissue engineering and in vitro modeling. *Gels*, 9(2), 132.

Mudgil, D. (2017). Chapter 3-The interaction between insoluble and soluble fiber In: Samaan, RA, editor. Dietary fiber for the prevention of cardiovascular disease. London, UK: Academic Press.

Murphy, S. V. & Atala, A. (2014). 3D bioprinting of tissues and organs. *Nature biotechnology*, 32(8), 773–785.

Murray, B. S. (2007). Stabilization of bubbles and foams. *Current Opinion in Colloid & Interface Science*, 12(4-5), 232–241.

Ning, L., Mehta, R., Cao, C., Theus, A., Tomov, M., Zhu, N., Weeks, E. R., Bauser-Heaton, H. & Serpooshan, V. (2020). Embedded 3D bioprinting of gelatin methacryloyl-based constructs with highly tunable structural fidelity. *ACS applied materials & interfaces*, 12(40), 44563–44577.

Noor, N., Shapira, A., Edri, R., Gal, I., Wertheim, L. & Dvir, T. (2019). 3D printing of personalized thick and perfusable cardiac patches and hearts. *Advanced science*, 6(11), 1900344.

O'brien, F. J. (2011). Biomaterials & scaffolds for tissue engineering. *Materials today*, 14(3), 88–95.

Olson, J. L., Atala, A. & Yoo, J. J. (2011). Tissue engineering: current strategies and future directions. *Chonnam medical journal*, 47(1), 1–13.

Osidak, E. O., Kozhukhov, V. I., Osidak, M. S. & Domogatsky, S. P. (2020). Collagen as bioink for bioprinting: a comprehensive review. *International journal of bioprinting*, 6(3), 270.

Ott, H. C., Matthiesen, T. S., Goh, S.-K., Black, L. D., Kren, S. M., Netoff, T. I. & Taylor, D. A. (2008). Perfusion-decellularized matrix: using nature's platform to engineer a bioartificial heart. *Nature medicine*, 14(2), 213–221.

Ouyang, L., Highley, C. B., Sun, W. & Burdick, J. A. (2017). A generalizable strategy for the 3D bioprinting of hydrogels from nonviscous photo-crosslinkable inks. *Advanced materials*, 29(8), 1604983.

Ozbolat, I. T. & Hospodiuk, M. (2016). Current advances and future perspectives in extrusion-based bioprinting. *Biomaterials*, 76, 321–343.

Park, J. A., Lee, Y. & Jung, S. (2023). Inkjet-based bioprinting for tissue engineering. *Organoid*, 3.

Parmar, P. A., Skaalure, S. C., Chow, L. W., St-Pierre, J.-P., Stoichevska, V., Peng, Y. Y., Werkmeister, J. A., Ramshaw, J. A. & Stevens, M. M. (2016). Temporally degradable collagen–mimetic hydrogels tuned to chondrogenesis of human mesenchymal stem cells. *Biomaterials*, 99, 56–71.

Pitois, O. (2012). Foam ripening. *Foam engineering: fundamentals and applications*, 59–73.

Poornejad, N., Momtahan, N., Salehi, A. S., Scott, D. R., Fronk, C. A., Roeder, B. L., Reynolds, P. R., Bundy, B. C. & Cook, A. D. (2016). Efficient decellularization of whole porcine kidneys improves reseeded cell behavior. *Biomedical Materials*, 11(2), 025003.

Rahimnejad, M., Adoungotchodo, A., Demarquette, N. R. & Lerouge, S. (2022). FRESH bioprinting of biodegradable chitosan thermosensitive hydrogels. *Bioprinting*, 27, e00209.

Ramesh, S., Harrysson, O. L., Rao, P. K., Tamayol, A., Cormier, D. R., Zhang, Y. & Rivero, I. V. (2021). Extrusion bioprinting: Recent progress, challenges, and future opportunities. *Bioprinting*, 21, e00116.

Ravanbakhsh, H., Karamzadeh, V., Bao, G., Mongeau, L., Juncker, D. & Zhang, Y. S. (2021). Emerging technologies in multi-material bioprinting. *Advanced Materials*, 33(49), 2104730.

Ribezzi, D., Gueye, M., Florczak, S., Dusi, F., de Vos, D., Manente, F., Hierholzer, A., Fussenegger, M., Caiazzo, M., Blunk, T. et al. (2023). Shaping synthetic multicellular and complex multimaterial tissues via embedded extrusion-volumetric printing of microgels. *Advanced Materials*, 35(36), 2301673.

Rocca, M., Fragasso, A., Liu, W., Heinrich, M. A. & Zhang, Y. S. (2018). Embedded multimaterial extrusion bioprinting. *SLAS TECHNOLOGY: Translating Life Sciences Innovation*, 23(2), 154–163.

Roosens, A., Somers, P., De Somer, F., Carriel, V., Van Nooten, G. & Cornelissen, R. (2016). Impact of detergent-based decellularization methods on porcine tissues for heart valve engineering. *Annals of biomedical engineering*, 44(9), 2827–2839.

Rouchi, A. H. & Mahdavi-Mazdeh, M. (2015). Regenerative medicine in organ and tissue transplantation: shortly and practically achievable? *International journal of organ transplantation medicine*, 6(3), 93.

Sadahira, M. S., Lopes, F. C. R., Rodrigues, M. I., Yamada, A. T., Cunha, R. L. & Netto, F. M. (2015). Effect of pH and interaction between egg white protein and hydroxypropymethylcellulose in bulk aqueous medium on foaming properties. *Carbohydrate polymers*, 125, 26–34.

Saini, G., Segaran, N., Mayer, J. L., Saini, A., Albadawi, H. & Oklu, R. (2021). Applications of 3D bioprinting in tissue engineering and regenerative medicine. *Journal of clinical medicine*, 10(21), 4966.

Schmidt, I., Novales, B., Boué, F. & Axelos, M. A. (2010). Foaming properties of protein/pectin electrostatic complexes and foam structure at nanoscale. *Journal of colloid and interface science*, 345(2), 316–324.

Schwab, A., Levato, R., D'este, M., Piluso, S., Eglin, D. & Malda, J. (2020). Printability and shape fidelity of bioinks in 3D bioprinting. *Chemical reviews*, 120(19), 11028–11055.

Shapira, A., Noor, N., Asulin, M. & Dvir, T. (2018). Stabilization strategies in extrusion-based 3D bioprinting for tissue engineering. *Applied Physics Reviews*, 5(4).

Shapira, A., Noor, N., Oved, H. & Dvir, T. (2020). Transparent support media for high resolution 3D printing of volumetric cell-containing ECM structures. *Biomedical Materials*, 15(4), 045018.

Shiwarski, D. J., Hudson, A. R., Tashman, J. W. & Feinberg, A. W. (2021). Emergence of FRESH 3D printing as a platform for advanced tissue biofabrication. *APL bioengineering*, 5(1).

Sill, T. J. & Von Recum, H. A. (2008). Electrospinning: applications in drug delivery and tissue engineering. *Biomaterials*, 29(13), 1989–2006.

Skylar-Scott, M. A., Uzel, S. G., Nam, L. L., Ahrens, J. H., Truby, R. L., Damaraju, S. & Lewis, J. A. (2019). Biomanufacturing of organ-specific tissues with high cellular density and embedded vascular channels. *Science advances*, 5(9), eaaw2459.

Song, K. H., Highley, C. B., Rouff, A. & Burdick, J. A. (2018). Complex 3D-printed microchannels within cell-degradable hydrogels. *Advanced Functional Materials*, 28(31), 1801331.

Sultana, N. (2023). Biological properties and biomedical applications of pectin and pectin-based composites: A review. *Molecules*, 28(24), 7974.

Taghizadeh, M., Taghizadeh, A., Yazdi, M. K., Zarrintaj, P., Stadler, F. J., Ramsey, J. D., Habibzadeh, S., Rad, S. H., Naderi, G., Saeb, M. R. et al. (2022). Chitosan-based inks for 3D printing and bioprinting. *Green Chemistry*, 24(1), 62–101.

Tong, A. & Voronov, R. (2022). A minireview of microfluidic scaffold materials in tissue engineering. *Frontiers in Molecular Biosciences*, 8, 783268.

Toniazzo, T. & Fabi, J. P. (2023). Versatile polysaccharides for application to semi-solid and fluid foods: The pectin case. *Fluids*, 8(9), 243.

Touani, F. K., Hamouda, I., Noiseux, N., Hoesli, C., Der Sarkissian, S. & Lerouge, S. (2025). Injectable, cryopreservable mesenchymal stromal cell-loaded microbeads for pro-angiogenic therapy: in vitro proof-of-concept. *Biomedical Materials*, 20(1), 015041.

Vacanti, J. P. & Langer, R. (1999). Tissue engineering: the design and fabrication of living replacement devices for surgical reconstruction and transplantation. *The lancet*, 354, S32–S34.

Vacanti, R. L. & Langer, J. P. (1993). Tissue Engineering. *Science*, 260(5110), 920–926. doi: 10.1126/science.8493529.

Villata, S., Frascella, F., Gaglio, C. G., Nastasi, G., Petretta, M., Pirri, C. F. & Baruffaldi, D. (2024). Self-standing gelatin-methacryloyl 3D structure using Carbopol-embedded printing. *Journal of Polymer Science*, 62(11), 2259–2269.

Wang, Q., Chen, K., Zhang, Y., Shao, F., Tan, X., Ying, Q., Wang, L., Ren, C., Zhang, L. & Wang, H. (2025). Nanostructured GelMA colloidal gels as bioinks for freeform multi-mode 3D printing: better replacement for the classical GelMA polymeric inks. *Bioactive Materials*, 53, 188–204.

Wang, X., Ao, Q., Tian, X., Fan, J., Tong, H., Hou, W. & Bai, S. (2017). Gelatin-based hydrogels for organ 3D bioprinting. *Polymers*, 9(9), 401.

Wei, Q., Young, J., Holle, A., Li, J., Bieback, K., Inman, G., Spatz, J. P. & Cavalcanti-Adam, E. A. (2020). Soft hydrogels for balancing cell proliferation and differentiation. *ACS biomaterials science & engineering*, 6(8), 4687–4701.

Wu, D. T., Jeffreys, N., Diba, M. & Mooney, D. J. (2022). Viscoelastic biomaterials for tissue regeneration. *Tissue Engineering Part C: Methods*, 28(7), 289–300.

Wu, W., DeConinck, A. & Lewis, J. A. (2011). Omnidirectional printing of 3D microvascular networks. *Advanced materials*, 23(24), H178–H183.

Xia, B. & Chen, G. (2022). Research progress of natural tissue-derived hydrogels for tissue repair and reconstruction. *International Journal of Biological Macromolecules*, 214, 480–491.

Xu, X., Jha, A. K., Harrington, D. A., Farach-Carson, M. C. & Jia, X. (2012). Hyaluronic acid-based hydrogels: from a natural polysaccharide to complex networks. *Soft matter*, 8(12), 3280–3294.

Yadav, M., Kaushik, B., Rao, G. K., Srivastava, C. M. & Vaya, D. (2023). Advances and challenges in the use of chitosan and its derivatives in biomedical fields: A review. *Carbohydrate Polymer Technologies and Applications*, 5, 100323.

Yang, B., Liu, T., Gao, G., Zhang, X. & Wu, B. (2022). Fabrication of 3D GelMA scaffolds using agarose microgel embedded printing. *Micromachines*, 13(3), 469.

Yogeshwaran, S., Hosseinabadi, H. G., Gendy, D. E. & Miri, A. K. (2024). Design considerations and biomaterials selection in embedded extrusion 3D bioprinting. *Biomaterials Science*, 12(18), 4506–4518.

Zeng, X., Meng, Z., He, J., Mao, M., Li, X., Chen, P., Fan, J. & Li, D. (2022). Embedded bioprinting for designer 3D tissue constructs with complex structural organization. *Acta biomaterialia*, 140, 1–22.

Zhan, F., Youssef, M., Shah, B. R., Li, J. & Li, B. (2022). Overview of foam system: Natural material-based foam, stabilization, characterization, and applications. *Food Hydrocolloids*, 125, 107435.

Zhang, C., Hua, W., Mitchell, K., Raymond, L., Delzendehrooy, F., Wen, L., Do, C., Chen, J., Yang, Y., Linke, G. et al. (2024). Multiscale embedded printing of engineered human tissue and organ equivalents. *Proceedings of the National Academy of Sciences*, 121(9), e2313464121.

Zhang, H., Wang, Y., Zheng, Z., Wei, X., Chen, L., Wu, Y., Huang, W. & Yang, L. (2023a). Strategies for improving the 3D printability of decellularized extracellular matrix bioink. *Theranostics*, 13(8), 2562.

Zhang, S., Waterhouse, G. I., Xu, F., He, Z., Du, Y., Lian, Y., Wu, P. & Sun-Waterhouse, D. (2023b). Recent advances in utilization of pectins in biomedical applications: A review focusing on molecular structure-directing health-promoting properties. *Critical Reviews in Food Science and Nutrition*, 63(19), 3386–3419.

Zhu, J., Zheng, N., Yang, Z., Li, X. & Lei, T. (2023). Experimental study on the foam-stabilizing advantages and foam stabilization mechanism of novel microbial polysaccharides. *Journal of Molecular Liquids*, 385, 122428.

Zumdahl, S. & Zumdahl, S. (2000). *Chemistry* (ed. 5th). Boston, MA: Houghton Mifflin Company.